

# Spatial Sign based Principal Component Analysis for High Dimensional Data

Long Feng<sup>1</sup>

<sup>1</sup>School of Statistics and Data Science, KLMDASR, LEBPS, and LPMC,  
Nankai University

## Abstract

This article focuses on the robust principal component analysis (PCA) of high-dimensional data with elliptical distributions. We investigate the PCA of the sample spatial-sign covariance matrix in both nonsparse and sparse contexts, referring to them as SPCA and SSPCA, respectively. We present both nonasymptotic and asymptotic analyses to quantify the theoretical performance of SPCA and SSPCA. In sparse settings, we demonstrate that SSPCA, implemented through a combinatoric program, achieves the optimal rate of convergence. Our proposed SSPCA method is computationally efficient and exhibits robustness against heavy-tailed distributions compared to existing methods. Simulation studies and real-world data applications further validate the superiority of our approach.

*Keywords:* Elliptical distribution; High dimensional data; Sparse principal component analysis; Spatial-sign covariance matrix.

## 1 Introduction

PCA (Principal Component Analysis) is a widely used statistical method for data dimensionality reduction. It transforms high-dimensional data into a lower-dimensional space

while preserving as much of the original data’s variability as possible. PCA achieves this by identifying the directions of maximum variance in the data, known as principal components, and projecting the data onto these directions. This process removes redundant information and noise, making the data easier to handle and visualize. PCA is commonly applied in fields such as machine learning, image processing, and finance, where dealing with high-dimensional data is common.

The classical PCA method can encounter significant difficulties when the number of input variables  $p$  is not substantially smaller than the sample size  $n$ . Specifically, PCA becomes inconsistent when the ratio  $p/n$  converges to some  $\gamma$  within the interval  $(0, 1)$ , as noted by Johnstone and Lu (2009). Furthermore, PCA’s performance deteriorates even more dramatically when  $p$  is significantly larger than  $n$ . To address this challenge, we invoke the assumption of sparsity. One form of sparsity assumption pertains to the spectrum of the covariance matrix, as explored in works such as Johnstone and Lu (2009), Baik and Silverstein (2006), Paul (2007), Nadler (2008), Birnbaum et al. (2013), and Cai et al. (2013). Another, more widely adopted assumption, focuses on the sparsity of the eigenvectors of the covariance matrix. Sparsity in the loadings offers a distinct advantage in interpretability, as it implies that each principal component is influenced by a limited subset of input variables. In this study, we focus on this latter assumption.

In the context of sparse settings, numerous sparse PCA methods have been explored in the literature. Jolliffe et al. (2003) and Zou et al. (2006) approached principal component analysis as a regression-type optimization problem and incorporated lasso-type penalties for parameter estimation. Shen and Huang (2008) and Witten et al. (2009) leveraged the relationship between PCA and singular value decomposition (SVD) to extract sparse loadings through iterative thresholding. Journee et al. (2010) introduced Gpower, a generalized power method for sparse PCA, by reformulating PCA with sparsity-inducing penalties as the maximization of a convex function over a sphere. Zhang and El Ghaoui (2011) proposed a greedy search algorithm for finding principal submatrices of the covariance matrix. Vu et al. (2013) formulated the sparse principal subspace problem as a semidefinite program with a Fantope

constraint and developed the Fantope Projection and Selection (FPS) algorithm to solve it. Ma (2013) and Yuan and Zhang (2013) suggested modified versions of the power method for estimating eigenvectors and principal subspaces. For a thorough overview of sparse PCA, readers are referred to Zou and Xue (2018).

One limitation of the aforementioned PCA and sparse PCA methods is their reliance on the assumption of Gaussian or sub-Gaussian distributions. When observations exhibit heavy-tailed behavior, these estimators may not be consistent. To tackle this problem, numerous studies have proposed replacing the sample covariance matrix with a robust covariance matrix. Examples include the works of Hubert et al. (2005), Croux et al. (2013), Han and Liu (2014), Hubert et al. (2016), Han and Liu (2018). These approaches aim to enhance the robustness of PCA and sparse PCA methods by utilizing robust covariance matrices that are less sensitive to outliers and heavy-tailed distributions. Specially, Han and Liu (2014) employed the marginal Kendall’s tau statistic to estimate the correlation matrix under the semiparametric transelliptical family. However, as highlighted in Han and Liu (2018), this method has two primary drawbacks: it only estimates the correlation matrix rather than the covariance matrix, and the sign sub-Gaussian condition is not straightforward to verify. To overcome these limitations, Han and Liu (2018) proposed using the multivariate Kendall’s tau matrix as a substitute for the sample covariance matrix to estimate eigenvectors under the elliptical model and various settings.

Under the assumption of an elliptical distribution, Marden (1999) demonstrated that both the population multivariate Kendall’s tau matrix and the spatial-sign covariance matrix share the same eigenspace as the covariance matrix. Consequently, these two matrices have been widely used in the literature to estimate principal components in low-dimensional settings. Notable contributions include the works of Locantore et al. (1999), Marden (1999), Visuri et al. (2000), Croux et al. (2002), Taskinen et al. (2012). It is important to note that the population multivariate Kendall’s tau matrix is equivalent to the population spatial-sign covariance matrix. However, when considering their sample counterparts, the computational complexity of the sample multivariate Kendall’s tau matrix ( $n^2 d^2$ ) is significantly higher than

that of the sample spatial-sign covariance matrix ( $nd^2$ ), particularly for large sample sizes. Therefore, it is of great interest to analyze the performance of the principal component estimator using the sample spatial-sign covariance matrix in high-dimensional scenarios.

For elliptical distributions, classic spatial-sign-based procedures have proven to be highly robust and efficient in traditional multivariate analysis, as overviewed by Oja (2010). Recent literature has also shown that these spatial-sign-based procedures excel in high-dimensional settings. Specifically, Wang et al. (2015), Feng and Sun (2016), and Feng et al. (2021) have proposed spatial-sign-based test procedures for the high-dimensional one-sample location problem. Additionally, Feng et al. (2016) and Huang et al. (2023) have addressed the high-dimensional two-sample location problem using spatial-sign-based methods. Moreover, Zou et al. (2014), Feng and Liu (2017) and Zhang et al. (2022) extended the spatial-sign-based method to the high-dimensional sphericity test, while Paindaveine and Verdebout (2016) and Zhao et al. (2023) considered high-dimensional white noise tests.

In this paper, we investigate principal component analysis using the spatial-sign covariance matrix in high-dimensional settings. Firstly, we establish theoretical results for Spatial-sign based Principal Component Analysis (SPCA) in the nonsparse scenario. We demonstrate that the rate of convergence of the eigenvector comprises two components: one is comparable to that of the Elliptical Component Analysis (ECA) proposed by (Han and Liu, 2018), i.e.,  $O_p(\sqrt{r^*(\Sigma) \log d/n})$ , and the other is influenced by the consistency of the spatial median. This is not unexpected, as the sample spatial-sign covariance matrix requires the estimation of the location parameter, whereas the sample multivariate Kendall's tau matrix does not. Fortunately, under certain mild conditions, we can show that the second component is of a smaller order compared to the first. Secondly, in the sparse setting, we propose a Sparse Spatial-sign based Principal Component Analysis (SSPCA) through a combinatorial program and demonstrate that it can achieve the minimax optimal rate of convergence. Thirdly, we present a computationally efficient algorithm based on the truncated power method proposed by (Yuan and Zhang, 2013). We also consider two initial estimators. One is the simple eigenvectors of the sample spatial-sign covariance matrix, which is very

easily computed. The other is using the Fantope projectoin (Vu et al., 2013). Lastly, we also provide a procedure for estimating the tuning parameter that controls the sparsity level.

Simulation studies indicate that our proposed methods exhibit robustness in handling heavy-tailed distributions. When compared to ECA, our SSPCA not only computes more rapidly but also demonstrates greater efficiency. These findings align with those reported in Feng (2018), which suggest that rank-based methods are less efficient than sign-based methods in high-dimensional contexts. Furthermore, our newly proposed method for determining the number of nonzero components in eigenvectors remains consistent as sample sizes increase. Applications to real data further underscore the advantages of our approach.

The remainder of this article is structured as follows. Section 2 introduces SPCA in non-sparse settings, while Section 3 presents the SSPCA method in sparse settings. Simulation studies are discussed in Section 4, and real data applications are examined in Section 5. Section 6 concludes the article, and all the detailed proofs are provided in the Appendix.

*Notation:* Here we use the same notations as Han and Liu (2018). Let  $\mathbf{M} = [\mathbf{M}_{jk}] \in \mathbb{R}^{d \times d}$  be a symmetric matrix and  $\mathbf{v} = (v_1, \dots, v_d)^T \in \mathbb{R}^d$  be a vector. We denote  $\mathbf{v}_I$  to be the subvector of  $\mathbf{v}$  whose entries are indexed by a set  $I$ , and  $\mathbf{M}_{I,J}$  to be the submatrix of  $\mathbf{M}$  whose rows are indexed by  $I$  and columns are indexed by  $J$ . We denote  $\text{supp}(\mathbf{v}) := \{j : v_j \neq 0\}$ . For  $0 < q < \infty$ , we define the  $\ell_q$  and  $\ell_\infty$  vector norms as  $\|\mathbf{v}\|_q := \left(\sum_{i=1}^d |v_i|^q\right)^{1/q}$  and  $\|\mathbf{v}\|_\infty := \max_{1 \leq i \leq d} |v_i|$ . We denote  $\|\mathbf{v}\|_0 := \text{card}(\text{supp}(\mathbf{v}))$ . We define the matrix entry-wise maximum value and Frobenius norms as  $\|\mathbf{M}\|_{\max} := \max\{|\mathbf{M}_{ij}|\}$  and  $\|\mathbf{M}\|_F = \left(\sum \mathbf{M}_{jk}^2\right)^{1/2}$ . Let  $\lambda_j(\mathbf{M})$  be the  $j$  th largest eigenvalue of  $\mathbf{M}$ . If there are ties,  $\lambda_j(\mathbf{M})$  is any one of the eigenvalues such that any eigenvalue larger than it has rank smaller than  $j$ , and any eigenvalue smaller than it has rank larger than  $j$ . Let  $\mathbf{u}_j(\mathbf{M})$  be any unit vector  $\mathbf{v}$  such that  $\mathbf{v}^T \mathbf{M} \mathbf{v} = \lambda_j(\mathbf{M})$ . Without loss of generality, we assume that the first nonzero entry of  $\mathbf{u}_j(\mathbf{M})$  is positive. We denote  $\|\mathbf{M}\|_2$  to be the spectral norm of  $\mathbf{M}$  and  $\mathbb{S}^{d-1} := \{\mathbf{v} \in \mathbb{R}^d : \|\mathbf{v}\|_2 = 1\}$  to be the  $d$ -dimensional unit sphere. We define the restricted spectral norm  $\|\mathbf{M}\|_{2,s} := \sup_{\mathbf{v} \in \mathbb{S}^{d-1}, \|\mathbf{v}\|_0 \leq s} |\mathbf{v}^T \mathbf{M} \mathbf{v}|$ , so for  $s = d$ , we have  $\|\mathbf{M}\|_{2,s} = \|\mathbf{M}\|_2$ . We denote  $f(\mathbf{M})$  to be the matrix with entries  $[f(\mathbf{M})]_{jk} = f(\mathbf{M}_{jk})$ . We denote  $\text{diag}(\mathbf{M})$  to be the diagonal matrix with

the same diagonal entries as  $\mathbf{M}$ . Let  $\mathbf{I}_d$  represent the  $d$  by  $d$  identity matrix. For any two numbers  $a, b \in \mathbb{R}$ , we denote  $a \wedge b := \min\{a, b\}$  and  $a \vee b := \max\{a, b\}$ . For any two sequences of positive numbers  $\{a_n\}$  and  $\{b_n\}$ , we write  $a_n \asymp b_n$  if  $a_n = O(b_n)$  and  $b_n = O(a_n)$ . We write  $b_n = \Omega(a_n)$  if  $a_n = O(b_n)$ , and  $b_n = \Omega^o(a_n)$  if  $b_n = \Omega(a_n)$  and  $b_n \not\asymp a_n$ . For any random variable  $X \in \mathbb{R}$ , we define the sub-Gaussian ( $\|\cdot\|_{\psi_2}$ ) and sub-exponential norms ( $\|\cdot\|_{\psi_1}$ ) of  $X$  as follows:

$$\begin{aligned} \|X\|_{\psi_2} &:= \sup_{k \geq 1} k^{-1/2} (E|X|^k)^{1/k} \quad \text{and} \\ \|X\|_{\psi_1} &:= \sup_{k \geq 1} k^{-1} (E|X|^k)^{1/k}. \end{aligned}$$

Any  $d$ -dimensional random vector  $\mathbf{X} \in \mathbb{R}^d$  is said to be sub-Gaussian distributed with the sub-Gaussian constant  $\sigma$  if

$$\|\mathbf{v}^T \mathbf{X}\|_{\psi_2} \leq \sigma, \quad \text{for any } \mathbf{v} \in \mathbb{S}^{d-1}.$$

For any two vectors  $\mathbf{v}_1, \mathbf{v}_2 \in \mathbb{R}^d$ , let  $\sin \angle(\mathbf{v}_1, \mathbf{v}_2)$  be the sine of the angle between  $\mathbf{v}_1$  and  $\mathbf{v}_2$ , with

$$|\sin \angle(\mathbf{v}_1, \mathbf{v}_2)| := \sqrt{1 - (\mathbf{v}_1^T \mathbf{v}_2)^2}.$$

## 2 SPCA: Nonsparse Setting

Suppose  $d$ -dimensional random vector  $\mathbf{X}$  follows elliptical distribution  $EC_d(\boldsymbol{\mu}, \boldsymbol{\Sigma}, \xi)$ , i.e.

$$\mathbf{X} \stackrel{d}{=} \boldsymbol{\mu} + \xi \mathbf{A} \mathbf{U},$$

where  $\boldsymbol{\mu} \in \mathbb{R}^d$ ,  $\mathbf{U}$  is a uniform random vector on the unit sphere in  $\mathbb{R}^q$ ,  $\xi \geq 0$  is a scalar random variable independent of  $\mathbf{U}$ , and  $\mathbf{A} \in \mathbb{R}^{d \times q}$  is a deterministic matrix satisfying  $\mathbf{A} \mathbf{A}^T = \boldsymbol{\Sigma}$  and  $\boldsymbol{\Sigma} \in \mathbb{R}^{d \times d}$  with  $\text{rank}(\boldsymbol{\Sigma}) = q \leq d$ . Here,  $\boldsymbol{\Sigma}$  is called the scatter matrix. In this article, we only consider continuous elliptical distributions with  $P(\xi = 0) = 0$ . Similar to Han and Liu (2018), we also assume  $E(\xi^2) = q < \infty$  so that  $\text{Cov}(\mathbf{X}) = \boldsymbol{\Sigma}$ . In fact, our proposed methods still work even when  $E(\xi^2) = \infty$ .

The Spatial-Sign Covariance Matrix is defined as

$$\mathbf{S} \doteq E(U(\mathbf{X}_i - \boldsymbol{\mu})U(\mathbf{X}_i - \boldsymbol{\mu})^T) \quad (1)$$

where  $U(\mathbf{x}) = \mathbf{x}/\|\mathbf{x}\|I(\mathbf{x} \neq \mathbf{0})$  is the spatial sign function. By Theorem 4.4 in Oja (2010), we know that the eigenspace of the spatial sign covariance matrix  $\mathbf{S}$  is identical to the eigenspace of the covariance matrix  $\boldsymbol{\Sigma}$ . Note that, according to Lemma B.1 in Han and Liu (2018), we know that the multivariate Kendall's tau matrix. i.e.

$$\mathbf{K} = E(U(\mathbf{X}_i - \mathbf{X}_j)U(\mathbf{X}_i - \mathbf{X}_j)^T) \quad (2)$$

is equal to the spatial sign covariance matrix  $\mathbf{S}$ . So by Proposition 2.1 in Han and Liu (2018), the eigenvalues of  $\mathbf{S}$  is

$$\lambda_j(\mathbf{S}) = E\left(\frac{\lambda_j(\boldsymbol{\Sigma})Y_j^2}{\lambda_1(\boldsymbol{\Sigma})Y_1^2 + \dots + \lambda_q(\boldsymbol{\Sigma})Y_q^2}\right) \quad (3)$$

if  $\text{rank}(\mathbf{S}) = q$ , where  $\mathbf{Y} := (Y_1, \dots, Y_q)^T \sim N_q(\mathbf{0}, \mathbf{I}_q)$  is a standard multivariate Gaussian distribution. In addition,  $\mathbf{S}$  and  $\boldsymbol{\Sigma}$  share the same eigenspace with the same descending order of the eigenvalues. To estimate the spatial sign covariance matrix, we first need to estimate the location parameter  $\boldsymbol{\mu}$ . We often use the spatial median to estimate  $\boldsymbol{\mu}$ , i.e.

$$\hat{\boldsymbol{\mu}} = \arg \min_{\boldsymbol{\mu} \in \mathbb{R}^p} \sum_{i=1}^n \|\mathbf{X}_i - \boldsymbol{\mu}\|_2. \quad (4)$$

Then the sample spatial sign covariance matrix is defined as

$$\hat{\mathbf{S}} = \frac{1}{n} \sum_{i=1}^n U(\mathbf{X}_i - \hat{\boldsymbol{\mu}})U(\mathbf{X}_i - \hat{\boldsymbol{\mu}})^T \quad (5)$$

Visuri et al. (2000) show that the influence functions of the sample spatial sign covariance matrix are uniformly bounded, indicating their robustness. In fact, the influence function of the sample spatial sign covariance matrix at a distribution  $F$  symmetric around zero has the simple form

$$IF(\mathbf{x}, \hat{\mathbf{S}}, F) = U(\mathbf{x})U(\mathbf{x})^T - \hat{\mathbf{S}}$$

and is seen to be constant in the radius  $\|\mathbf{x}\|$  of the contamination point  $\mathbf{x}$ .

In this section, we first do not assume the sparsity of  $\mathbf{u}_1(\boldsymbol{\Sigma})$  and assume that  $\lambda_1(\boldsymbol{\Sigma})$  is distinct. Consequently, we propose the leading eigenvector of  $\hat{\mathbf{S}}$ , i.e.  $\mathbf{u}_1(\hat{\mathbf{S}})$  to estimate  $\mathbf{u}_1(\mathbf{S}) = \mathbf{u}_1(\boldsymbol{\Sigma})$ :

The *SPCA* (*Spatial-sign based Principal Component Analysis*) estimator:  $\mathbf{u}_1(\hat{\mathbf{S}})$  (the leading eigenvector of  $\hat{\mathbf{S}}$ ).

When the dimension  $d$  is fixed and  $\text{rank}(\boldsymbol{\Sigma}) = q$ , Croux et al. (2002) showed the asymptotic normality of  $\hat{\mathbf{u}}_1(\hat{\mathbf{S}})$ , i.e.

$$\sqrt{n}(\hat{\mathbf{u}}_1(\hat{\mathbf{S}}) - \mathbf{u}_1) \xrightarrow{d} N(0, \sigma_{u_1}^2)$$

where

$$\sigma_{u_1}^2 = \sum_{l \neq 1} \left[ \frac{\lambda_l(\boldsymbol{\Sigma}) \lambda_1(\boldsymbol{\Sigma}) b_{1l}}{(c_1 \lambda_1(\boldsymbol{\Sigma}) - c_l \lambda_l(\boldsymbol{\Sigma}))^2} \mathbf{u}_l \mathbf{u}_l^T \right]$$

where

$$c_l = E [u_1^2 / (\gamma_1 u_1^2 + \dots + \gamma_q u_q^2)]$$

for  $l = 1, \dots, q$ , and for  $1 \leq j, l \leq q$

$$b_{1l} = E [u_1^2 u_l^2 / (\gamma_1 u_1^2 + \dots + \gamma_q u_q^2)]^2$$

with  $(u_1, \dots, u_q)$  the components of a random variable  $\mathbf{u}$ , uniformly distributed on the periphery of a unit sphere, and  $\gamma_1, \dots, \gamma_p$  the standardized eigenvalues, that is  $\gamma_j(\boldsymbol{\Sigma}) = \lambda_j(\boldsymbol{\Sigma}) / (\lambda_1(\boldsymbol{\Sigma}) + \dots, \lambda_q(\boldsymbol{\Sigma}))$ .

To the best of our knowledge, as the dimension  $d$  approaches infinity, there are currently no asymptotic results available for  $\hat{\mathbf{u}}_1(\hat{\mathbf{S}})$ . So we first analysis the convergence rate of  $\mathbf{u}_1(\hat{\mathbf{S}})$  in high dimensional settings. According to Davis-Kahan inequality (Davis and Kahan, 1970; Wedin, 1972), to evaluate the convergence rate of  $\mathbf{u}_1(\hat{\mathbf{S}})$  to  $\mathbf{u}_1(\mathbf{S})$ , we first study the convergence rate of  $\hat{\mathbf{S}}$  to  $\mathbf{S}$  under the spectral norm.

Define  $\zeta_k = E(r_i^{-k})$ ,  $r_i = \|\mathbf{X}_i - \boldsymbol{\mu}\|$ ,  $\nu_i = \zeta_1^{-1} r_i^{-1}$ . We assume that

(A1)  $\zeta_k \zeta_1^{-k} < \zeta \in (0, \infty)$  for  $k = 1, 2, 3, 4$  and all  $d$ .

(A2)  $\limsup_d \|\mathbf{S}\|_2 < 1 - \psi < 1$  for some positive constant  $\psi$ .



Assumption (A1) is widely assumed in high dimensional spatial-sign based procedures, such as Zou et al. (2014), Feng et al. (2016). By condition (A1), we have  $E(\nu_i) = 1$ ,  $\sigma_\nu^2 = \text{Var}(\nu_i) < \zeta - 1$ ,  $\kappa_\nu = E(\nu_i^4) < \zeta$ . Assumption (A2) means that the maximum eigenvalue of  $\mathbf{S}$  should be uniformly smaller than one, which is employed to guarantee the consistency of the spatial median. In the past decades, there are some literatures which established the consistency of the spatial median under different assumptions, such as Zou et al. (2014), Cheng et al. (2019), Li and Xu (2022). However, all the above papers need to assume the eigenvalues of  $\mathbf{\Sigma}$  are all bounded or  $\text{tr}(\mathbf{\Sigma}^4) = o(\text{tr}^2(\mathbf{\Sigma}^2))$ , which is too restrictive in principal component analysis. In contrast, Assumption (A2) is less stringent than these prior assumptions.

Let  $r^*(\mathbf{S}) = \text{tr}(\mathbf{S})/\|\mathbf{S}\|_2 = \frac{1}{\lambda_1(\mathbf{S})}$ , which is referred to as the effective rank of  $\mathbf{S}$  in the literature (Vershynin, 2010; Lounici, 2014). The next theorem establish the convergence rate of  $\|\hat{\mathbf{S}} - \mathbf{S}\|_2$ .

**THEOREM 2.1** *Let  $\mathbf{X}_1, \dots, \mathbf{X}_n$  be  $n$  independent observations of  $\mathbf{X} \sim EC_d(\boldsymbol{\mu}, \mathbf{\Sigma}, \xi)$ . Let  $\hat{\mathbf{S}}$  be the sample version of the spatial-sign covariance matrix defined in Equation (5). We have, for any  $\alpha > 0$ , there exist a positive constant  $C_S$ , such that, for sufficient large  $n$  and any  $\delta \in (0, 1)$ ,*

$$\|\hat{\mathbf{S}} - \mathbf{S}\|_2 \leq \|\mathbf{S}\|_2 \sqrt{\frac{4(1 + r^*(\mathbf{S}))(\log d + \log(1/\alpha))}{n}} + C_S n^{-\frac{1}{2}(1+\delta)} \quad (6)$$

*with probability larger than  $1 - \alpha$ .*

The initial term in (6) bears a resemblance to the nonasymptotic bound for  $\|\hat{\mathbf{K}} - \mathbf{K}\|$  presented in Theorem 3.1 of Han and Liu (2018). Here,  $\hat{\mathbf{K}}$  represents the sample multivariate Kendall's tau estimator. Essentially, this term constitutes the nonasymptotic bound for  $\|\tilde{\mathbf{S}} - \mathbf{S}\|$ , where  $\tilde{\mathbf{S}} = \frac{1}{n} \sum_{i=1}^n U(\mathbf{X}_i - \boldsymbol{\mu})U(\mathbf{X}_i - \boldsymbol{\mu})^T$ . This result is established using the matrix Bernstein inequality introduced by Tropp (2012). The second term in (6) arises from the convergence rate of the spatial median. A key distinction between the two estimators of  $\mathbf{S} = \mathbf{K}$ , namely  $\hat{\mathbf{K}}$  and  $\hat{\mathbf{S}}$ , lies in the necessity to estimate the location parameter for  $\hat{\mathbf{S}}$ . This additional step introduces complexity to the proof of its convergence rate. Conversely,

the theoretical analysis of  $\widehat{\mathbf{K}}$  is simplified by obviating the need to estimate the location parameter. However, this simplification comes at the cost of increased computational burden, as  $\widehat{\mathbf{K}}$  is a second-order U-statistic, whereas  $\widehat{\mathbf{S}}$  is only a first-order U-statistic. Ultimately, if  $\frac{r^*(\mathbf{S})}{n^\delta \log d} \rightarrow 0$ , the second term will be of smaller order compared to the first term.

According to the Davis-Kahan inequality, we know that

$$\left| \sin \angle \left( \mathbf{u}_1(\widehat{\mathbf{S}}), \mathbf{u}_1(\mathbf{S}) \right) \right| \leq \frac{2}{\lambda_1(\mathbf{S}) - \lambda_2(\mathbf{S})} \|\widehat{\mathbf{S}} - \mathbf{S}\|_2.$$

So we can directly obtain the following corollary.

**COROLLARY 2.1** *Under the conditions of Theorem 2.1, for any  $\alpha > 0$ , there exist a positive constant  $C_S$ , such that, for sufficient large  $n$  and  $\delta \in (0, 1)$ , we have, with probability larger than  $1 - \alpha$ ,*

$$\begin{aligned} & \left| \sin \angle \left( \mathbf{u}_1(\widehat{\mathbf{S}}), \mathbf{u}_1(\mathbf{S}) \right) \right| \\ & \leq \frac{2\lambda_1(\mathbf{S})}{\lambda_1(\mathbf{S}) - \lambda_2(\mathbf{S})} \sqrt{\frac{4(r^*(\mathbf{S}) + 1)(\log d + \log(1/\alpha))}{n}} + \frac{2C_S}{\lambda_1(\mathbf{S}) - \lambda_2(\mathbf{S})} n^{-\frac{1}{2}(1+\delta)} \end{aligned}$$

If  $\lambda_1(\mathbf{S})/\lambda_2(\mathbf{S})$  is bounded by a constant, we need  $r^*(\mathbf{S}) \log d/n \rightarrow 0$  and  $r^*(\mathbf{S})n^{-\frac{1}{2}(1+\delta)} \rightarrow 0$  to make  $\mathbf{u}_1(\widehat{\mathbf{S}})$  a consistent estimator of  $\mathbf{u}_1(\mathbf{S})$ . If  $\log(d) = o(n^{\frac{1}{2}(1-\delta)})$ , we only need the assumption  $r^*(\mathbf{S}) \log d/n \rightarrow 0$ , which is consistent with the result in Han and Liu (2018). According to Theorem 3.2 in Han and Liu (2018),

$$r^*(\mathbf{S}) \leq \left( r^*(\mathbf{\Sigma}) + 4r^{**}(\mathbf{\Sigma})\sqrt{\log d} + 8 \log d \right) \left( 1 - \sqrt{3}d^{-2} \right)^{-1}$$

where  $r^{**}(\mathbf{\Sigma}) := \|\mathbf{\Sigma}\|_F/\lambda_1(\mathbf{\Sigma}) \leq \sqrt{d}$  is the ‘‘second-order’’ effective rank of the matrix  $\mathbf{\Sigma}$ . Additionally, if  $\|\mathbf{\Sigma}\|_F \log d = \text{tr}(\mathbf{\Sigma})$ , we have  $\lambda_j(\mathbf{S}) \asymp \lambda_j(\mathbf{\Sigma})/\text{tr}(\mathbf{\Sigma})$ . So

$$\frac{\lambda_1(\mathbf{S})}{\lambda_1(\mathbf{S}) - \lambda_2(\mathbf{S})} \asymp \frac{\lambda_1(\mathbf{\Sigma})}{\lambda_1(\mathbf{\Sigma}) - \lambda_2(\mathbf{\Sigma})}.$$

So, we can directly bound  $\|\widehat{\mathbf{S}} - \mathbf{S}\|_2$  and  $\left| \sin \angle \left( \mathbf{u}_1(\widehat{\mathbf{S}}), \mathbf{u}_1(\mathbf{S}) \right) \right|$  using  $\mathbf{\Sigma}$ .

We observe that Theorem 2.1 can also facilitate the quantification of the subspace estimation error through a variant of the Davis-Kahan inequality. Specifically, let  $\mathcal{P}^m(\widehat{\mathbf{S}})$  and

$\mathcal{P}^m(\mathbf{S})$  denote the projection matrices that map onto the subspaces spanned by the  $m$  leading eigenvectors of  $\widehat{\mathbf{S}}$  and  $\mathbf{S}$ , respectively. By invoking Lemma 4.2 from Vu and Lei (2013), we obtain the inequality:

$$\left\| \mathcal{P}^m(\widehat{\mathbf{S}}) - \mathcal{P}^m(\mathbf{S}) \right\|_{\text{F}} \leq \frac{2\sqrt{2m}}{\lambda_m(\mathbf{S}) - \lambda_{m+1}(\mathbf{S})} \|\widehat{\mathbf{S}} - \mathbf{S}\|_2,$$

which allows us to control  $\left\| \mathcal{P}^m(\widehat{\mathbf{S}}) - \mathcal{P}^m(\mathbf{S}) \right\|_{\text{F}}$  using a similar rationale as employed in Corollary 2.1.

### 3 Sparse SPCA: Sparse Setting

#### 3.1 Combinatoric Program

In this section, we consider sparse settings:  $\lambda_1(\boldsymbol{\Sigma})$  is distinct and  $\|\mathbf{u}_1(\boldsymbol{\Sigma})\|_0 \leq s < d \wedge n$ . For any matrix  $\mathbf{M} \in \mathbb{R}^{d \times d}$ , we define the best  $s$ -sparse vector approximating  $\mathbf{u}_1(\mathbf{M})$  as

$$\mathbf{u}_{1,s}(\mathbf{M}) := \arg \max_{\|\mathbf{v}\|_0 \leq s, \|\mathbf{v}\|_2 \leq 1} |\mathbf{v}^T \mathbf{M} \mathbf{v}| \quad (7)$$

We propose to estimate  $\mathbf{u}_1(\boldsymbol{\Sigma}) = \mathbf{u}_1(\mathbf{S})$  via a combinatoric program:

*Sparse SPCA estimator (SSPCA) via a combinatoric program* :  $\mathbf{u}_{1,s}(\widehat{\mathbf{S}})$ .

Similarly, to evaluate the performance of SSPCA, we first study the approximation error  $\|\widehat{\mathbf{S}} - \mathbf{S}\|_{2,s}$ .

**THEOREM 3.1** *Let  $\mathbf{X}_1, \dots, \mathbf{X}_n$  be  $n$  observations of  $\mathbf{X} \sim EC_d(\boldsymbol{\mu}, \boldsymbol{\Sigma}, \xi)$ , when  $(s \log(ed/s) + \log(1/\alpha))/n \rightarrow 0$ , with probability at least  $1 - 3\alpha$ , we have*

$$\|\widehat{\mathbf{S}} - \mathbf{S}\|_{2,s} \leq C_0 \left( \sup_{\mathbf{v} \in \mathbb{S}^{d-1}} 2 \|\mathbf{v}^T U(\mathbf{X})\|_{\psi_2}^2 + \|\mathbf{S}\|_2 \right) \sqrt{\frac{s(3 + \log(d/s)) + \log(1/\alpha)}{n}} + C_1 \left( \frac{nd}{s} \right)^{-\frac{1}{2}(1+\delta)}$$

for some absolute constants  $C_0, C_1 > 0$  and  $\delta \in (0, 1)$ . Specially, if  $\text{rank}(\boldsymbol{\Sigma}) = q$  and  $\|\mathbf{u}_1(\boldsymbol{\Sigma})\|_0 \leq s$ , we have

$$\|\widehat{\mathbf{S}} - \mathbf{S}\|_{2,s} \leq C_0 \left\{ \left( \frac{4\lambda_1(\boldsymbol{\Sigma})}{q\lambda_q(\boldsymbol{\Sigma})} \wedge 1 \right) + \lambda_1(\mathbf{S}) \right\} \sqrt{\frac{s(3 + \log(d/s)) + \log(1/\alpha)}{n}} + C_1 \left( \frac{nd}{s} \right)^{-\frac{1}{2}(1+\delta)}$$

The first term of the approximation error of  $\|\widehat{\mathbf{S}} - \mathbf{S}\|_{2,s}$  is the same as  $\|\widehat{\mathbf{K}} - \mathbf{K}\|_{2,s}$  by Theorem 4.1 and 4.2 in Han and Liu (2018). Similar to Theorem 2.1, the second term arises from the convergence rate of the spatial median. Under some special cases, such as condition number controlled (Bickel and Levina, 2008), spike covariance model (Johnstone and Lu, 2009), multi-factor model (Fan et al., 2008), Han and Liu (2018) showed that  $\sup_{\mathbf{v}} \|\mathbf{v}^T U(\mathbf{X})\|_{\psi_2}^2$  is of the same order as  $\lambda_1(\mathbf{S})$ . So the first term is  $O_P\left(\lambda_1(\mathbf{S})\sqrt{s \log(ed/s)/n}\right)$ . Then, if  $\frac{r^*(\mathbf{S})s^{\delta/2}}{n^{\delta/2}d^{\frac{1+\delta}{2}}\sqrt{\log(ed/s)}} \rightarrow 0$ , the second term is a smaller order than the first term.

By Davis-Kahan type inequality provided in Vu and Lei (2012), we have

$$\left| \sin \angle \left( \mathbf{u}_{1,s}(\widehat{\mathbf{S}}), \mathbf{u}_{1,s}(\mathbf{S}) \right) \right| \leq \frac{2}{\lambda_1(\mathbf{S}) - \lambda_2(\mathbf{S})} \|\widehat{\mathbf{S}} - \mathbf{S}\|_{2,2s}.$$

So we can directly obtain the following result.

**COROLLARY 3.1** *Under the condition of Theorem 3.1, if we have  $(s \log(ed/s) + \log(1/\alpha))/n \rightarrow 0$ , for  $n$  sufficiently large, with probability larger than  $1 - 2\alpha$ ,*

$$\begin{aligned} \left| \sin \angle \left( \mathbf{u}_{1,s}(\widehat{\mathbf{S}}), \mathbf{u}_{1,s}(\mathbf{S}) \right) \right| &\leq \frac{2C_0 (4\lambda_1(\mathbf{\Sigma})/q\lambda_q(\mathbf{\Sigma}) \wedge 1 + \lambda_1(\mathbf{S}))}{\lambda_1(\mathbf{S}) - \lambda_2(\mathbf{S})} \sqrt{\frac{2s(3 + \log(d/2s)) + \log(1/\alpha)}{n}} \\ &\quad + \frac{2C_1}{\lambda_1(\mathbf{S}) - \lambda_2(\mathbf{S})} \left( \frac{nd}{s} \right)^{-\frac{1}{2}(1+\delta)} \end{aligned}$$

By Wang et al. (2013), we have

$$\left\| \mathbf{U}_{m,s}(\widehat{\mathbf{S}})\mathbf{U}_{m,s}(\widehat{\mathbf{S}})^T - \mathbf{U}_{m,s}(\mathbf{S})\mathbf{U}_{m,s}(\mathbf{S})^T \right\|_{\text{F}} \leq \frac{2\sqrt{2m}}{\lambda_m(\mathbf{S}) - \lambda_{m+1}(\mathbf{S})} \cdot \|\widehat{\mathbf{S}} - \mathbf{S}\|_{2,2ms}$$

where

$$\mathbf{U}_{m,s}(\mathbf{M}) := \arg \max_{\mathbf{V} \in \mathbb{R}^{d \times m}} \langle \mathbf{M}, \mathbf{V}\mathbf{V}^T \rangle, \text{ subject to } \sum_{j=1}^d \mathbb{I}(\mathbf{V}_{j*} \neq \mathbf{0}) \leq s,$$

where  $\mathbf{V}_{j*}$  is the  $j$ th row of  $\mathbf{M}$  and the indicator function returns 0 if and only if  $\mathbf{V}_{j*} = \mathbf{0}$ . Then, the results obtained in Theorem 3.1 can also be used to bound the approximation error of the principal subspace estimation.

### 3.2 Computationally Efficient program

We adopt the truncated power algorithm proposed by Yuan and Zhang (2013) to solve the optimization problem (7). For any vector  $\mathbf{v} \in \mathbb{R}^d$  and an index set  $J \subset \{1, \dots, d\}$ , we define the truncation function  $\text{TRC}(\cdot, \cdot)$  to be

$$\text{TRC}(\mathbf{v}, J) := (v_1 \cdot \mathbb{I}(1 \in J), \dots, v_d \cdot \mathbb{I}(d \in J))^T$$

where  $\mathbb{I}(\cdot)$  is the indicator function. Algorithm 1 shows the detail procedures of our proposed SSPCA procedure.

---

#### Algorithm 1 Sparse Spatial-sign bases Principal Component Analysis (SSPCA)

---

**Require:** Matrix  $\hat{\mathbf{S}}$ , sparsity level  $k$ , convergence threshold  $\epsilon$

**Ensure:**  $\hat{\mathbf{u}}_{1,k}(\hat{\mathbf{S}})$

- 1: The initial parameter  $\mathbf{v}^{(0)}$ .
  - 2: **repeat**
  - 3:    $t \leftarrow t + 1$ .
  - 4:   Compute  $\mathbf{W}_t \leftarrow \hat{\mathbf{S}}\mathbf{v}^{(t-1)}$ .
  - 5:   **if**  $\|\mathbf{W}_t\|_0 \leq k$  **then**
  - 6:      $\mathbf{v}^{(t)} \leftarrow \mathbf{W}_t / \|\mathbf{W}_t\|_2$ .
  - 7:   **else**
  - 8:     Let  $A_t$  be the indices of the elements in  $\mathbf{W}_t$  with the  $k$  largest absolute values.
  - 9:      $\mathbf{v}^{(t)} \leftarrow \text{TRC}(\mathbf{W}_t, A_t) / \|\text{TRC}(\mathbf{W}_t, A_t)\|_2$ .
  - 10:   **end if**
  - 11: **until**  $\|\mathbf{v}^{(t)} - \mathbf{v}^{(t-1)}\|_2 \leq \epsilon$
  - 12:  $\hat{\mathbf{u}}_{1,k}(\hat{\mathbf{S}}) \leftarrow \mathbf{v}^{(t)}$ .
- 

The following theorem show the consistency of Algorithm 1, which is a directly result of Theorem 4 in Yuan and Zhang (2013). So we omit the detailed proof here.

**THEOREM 3.2** *Suppose  $\|\mathbf{v}^{(0)}\|_0 \leq s$  and  $\left|(\mathbf{v}^{(0)})^T \mathbf{u}_1(\mathbf{S})\right|$  is lower bounded by a positive constant  $C_3$ . Accordingly under the condition of Theorem 4 by Yuan and Zhang (2013), for*

$k \geq s$ , we have

$$\left| \sin \angle \left( \widehat{\mathbf{u}}_{1,k}(\widehat{\mathbf{S}}), \mathbf{u}_1(\mathbf{S}) \right) \right| = O_P \left( \sqrt{\frac{(k+s) \log d}{n}} \right).$$

In practical applications, we have observed that the leading eigenvector of  $\widehat{\mathbf{S}}$  exhibits excellent performance as an initial parameter. Therefore, we adopt this simpler initial estimator in our paper. Similar to the approach by Han and Liu (2018), the initial parameter  $\mathbf{v}^{(0)}$  can be estimated using the Fantope Projection method proposed by Vu et al. (2013). We introduce this method in the appendix.

### 3.3 Tuning parameter selection

The tuning parameter  $k$  in Algorithm 1 plays a crucial role in the performance of sparse PCA. A large value of  $k$  may result in the inclusion of numerous unimportant parameters, while a small value of  $k$  may lead to significant bias. One potential approach to selecting  $k$  is to utilize the criterion proposed by Yuan and Zhang (2013), which involves choosing the value of  $k$  that maximizes  $\left( \widehat{\mathbf{u}}_{1,k}(\widehat{\mathbf{S}}) \right)^T \cdot \widehat{\mathbf{S}}_{\text{val}} \cdot \widehat{\mathbf{u}}_{1,k}(\widehat{\mathbf{S}})$ , where  $\widehat{\mathbf{S}}_{\text{val}}$  represents an independent empirical spatial-sign covariance matrix calculated from a separate sample set of the data. Yuan and Zhang (2013) demonstrated that this heuristic approach performs well in practical applications. However, in situations where an independent sample set is not available, we recommend using the sample-split method as an alternative approach.

For each  $k$ , we randomly split the sample into two sets, denote the corresponding sample spatial-sign covariance matrix of each sample as  $\widehat{\mathbf{S}}_l^{(1)}$ ,  $\widehat{\mathbf{S}}_l^{(2)}$ , respectively. Then, we calculate

$$\hat{k} = \arg \max_{1 \leq k \leq K} \frac{1}{B} \sum_{l=1}^B \left( \widehat{\mathbf{u}}_{1,k}(\widehat{\mathbf{S}}_l^{(1)}) \right)^T \cdot \widehat{\mathbf{S}}_l^{(2)} \cdot \widehat{\mathbf{u}}_{1,k}(\widehat{\mathbf{S}}_l^{(1)}) \quad (8)$$

In the above discussion, we only consider estimate the leading eigenvector. To estimate more than one leading eigenvectors, we exploit the deflation method proposed by Mackey (2008). That is, we obtain multiple component estimates by taking the  $r$ -th component estimate  $\widehat{\mathbf{v}}_r$  from input matrix  $\mathbf{S}_r$ , and then re-running the method with the deflated input

matrix:  $\mathbf{S}_{r+1} = (\mathbf{I} - \hat{\mathbf{v}}_r \hat{\mathbf{v}}_r^T) \mathbf{S}_r (\mathbf{I} - \hat{\mathbf{v}}_r \hat{\mathbf{v}}_r^T)$ . The resulting  $m$ -dimensional principal subspace estimate is the span of  $\hat{\mathbf{v}}_1, \dots, \hat{\mathbf{v}}_m$ .

## 4 Simulation

### 4.1 Estimating Leading Eigenvector

We first consider estimating the leading eigenvector of the covariance matrix  $\Sigma$ . We consider the similar model for  $\Sigma$  as citehan2018eca, i.e.

$$\Sigma = \sum_{j=1}^m (\omega_j - \omega_d) \mathbf{v}_j \mathbf{v}_j^T + \omega_d \mathbf{I}_d$$

where  $\omega_1 > \omega_2 > \omega_3 = \dots = \omega_d$  be the eigenvalues and  $\mathbf{v}_1, \dots, \mathbf{v}_d$  be the eigenvectors of  $\Sigma$  with  $\mathbf{v}_j := (v_{j1}, \dots, v_{jd})^T$ . The top  $m$  leading eigenvectors  $\mathbf{v}_1, \dots, \mathbf{v}_m$  of  $\Sigma$  are specified to be sparse such that  $s_j := \|\mathbf{v}_j\|_0$  is small and

$$v_{jk} = \begin{cases} 1/\sqrt{s_j}, & 1 + \sum_{i=1}^{j-1} s_i \leq k \leq \sum_{i=1}^j s_i \\ 0, & \text{otherwise.} \end{cases}$$

In this subsection, we set  $m = 2$  and  $\omega_1 = 5, \omega_2 = 3, \omega_3 = \dots = \omega_p = 1$ . We consider the following three different elliptical distributions:

- (I) Multivariate normal distribution.  $\mathbf{X} \sim N(\boldsymbol{\theta}, \Sigma)$ .
- (II) Multivariate  $t$ -distribution  $t_{N,3}$ .  $\mathbf{X}$ 's are generated from standardized  $t_{N,3}/\sqrt{3}$  with mean zero and scatter matrix  $\Sigma$ .
- (III) Multivariate mixture normal distribution  $\text{MN}_{N,\kappa,9}$ .  $\mathbf{X}$ 's are generated from standardized  $[\kappa N(\mathbf{0}, \Sigma) + (1 - \kappa)N(\mathbf{0}, 9\Sigma)]/\sqrt{\kappa + 9(1 - \kappa)}$ , denoted by  $\text{MN}_{N,\gamma,9}$ .  $\kappa$  is chosen to be 0.8.

All the simulation results are based on 1000 replication. Figure 1 plots the averaged distances between the estimate  $\hat{\mathbf{v}}_1$  and  $\mathbf{v}_1$ , defined as  $|\sin \angle(\hat{\mathbf{v}}_1, \mathbf{v}_1)|$ , against the number of estimated nonzero entries (defined as  $\|\hat{\mathbf{v}}_1\|_0$ ), for three different methods:

- TP: Sparse PCA method on the Pearson’s sample covariance matrix (Yuan and Zhang, 2013);
- ECA: Elliptical component analysis based on the multivariate kendall’s tau matrix (Han and Liu, 2018).
- SSPCA: Sparse spatial-sign based Principal component analysis.

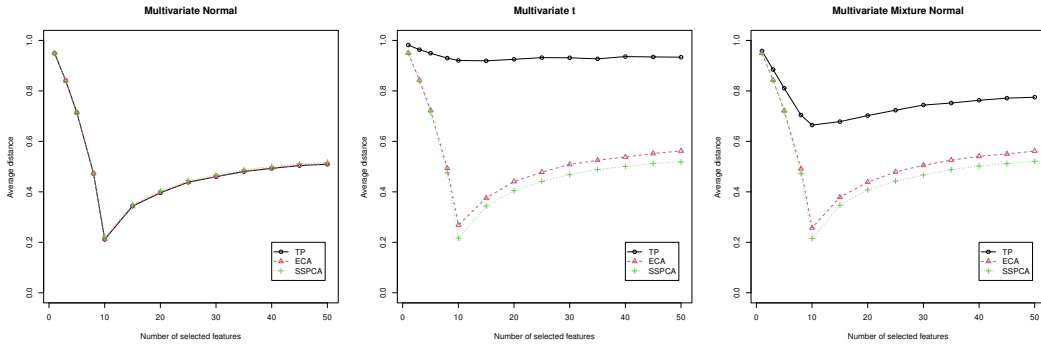
In this case, we set  $n = 100$  and varied  $d$  to be 100, 200, 300. Our findings indicate that SSPCA consistently outperforms ECA and TP in estimation accuracy. This result underscores the effectiveness of SSPCA in handling high-dimensional data with potential sparsity. SSPCA’s ability to accurately estimate the principal components in high-dimensional settings is a crucial advantage, as many modern datasets are characterized by a large number of features. Furthermore, when the data are indeed normally distributed, we observed no significant difference in performance between SSPCA, ECA, and TP. This observation suggests that SSPCA is a reliable alternative to sparse PCA within the elliptical family of distributions. The fact that SSPCA performs comparably to other methods in the case of normally distributed data, while also excelling in high-dimensional and sparse settings, demonstrates its versatility and robustness. Overall, these findings highlight the potential of SSPCA as a powerful tool for analyzing high-dimensional data in a variety of contexts.

To evaluate the dependence of the estimation accuracy of the SSPCA estimator on the triplet  $(n, d, s)$ , we conducted experiments with varying values of  $d$ ,  $s$ , and sample size  $n$ . Specifically, we considered  $d = 100, 200, 300$ ,  $s_1 = 5, 10, 20$ , and varying sample sizes  $n$ . The results, presented in Figure 2, show the curves of averaged distances between the estimates and true parameters. In these experiments, we set the number of selected features equal to the true parameter  $s$ . Our findings indicate that the averaged distance between  $\mathbf{v}_1$  and  $\hat{\mathbf{v}}_1$  approaches zero as the sample size increases, which demonstrates the consistency of our proposed SSPCA methods. This consistency is an important characteristic of any estimator, as it indicates that the estimates produced by the method will be increasingly accurate as more data is available. Additionally, we observed that all the curves in Figure

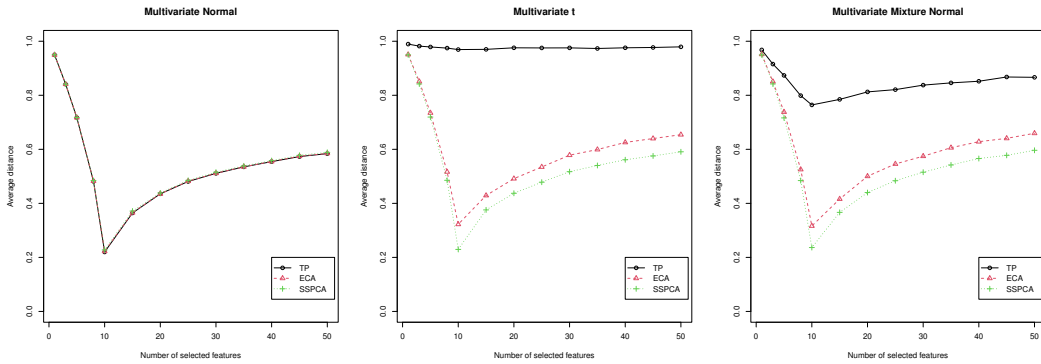


Figure 1: Curves of averaged distances between the estimates and true parameters with different number of selected features.

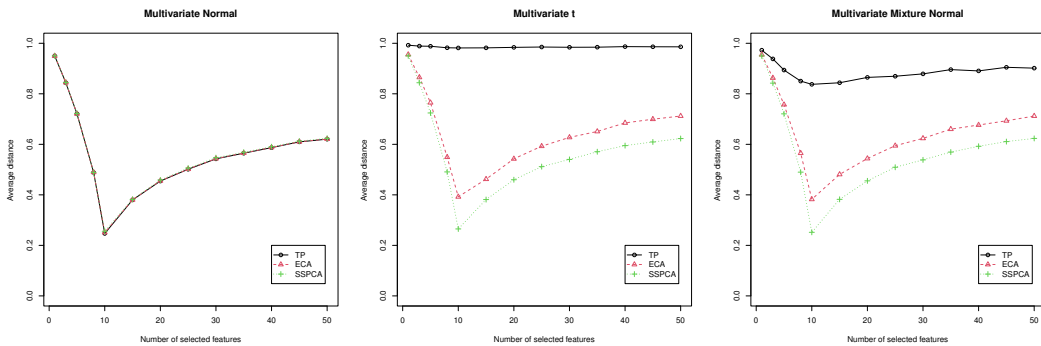
(a)  $n = 100, d = 100$



(b)  $n = 100, d = 200$



(c)  $n = 100, d = 300$



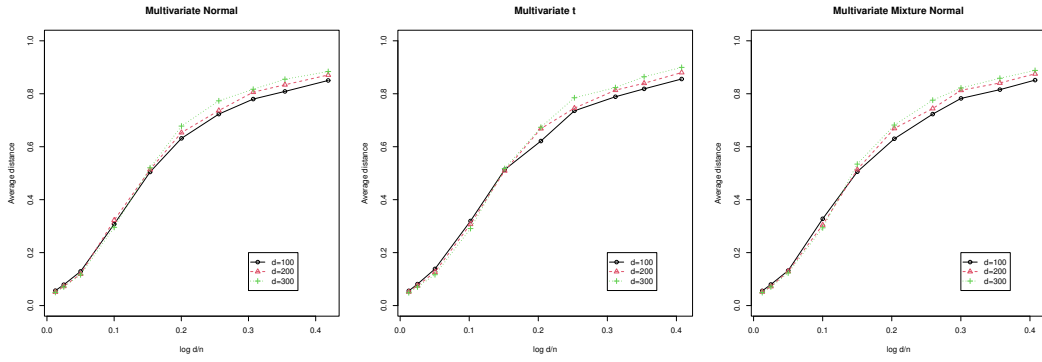
2 almost overlap with each other when the average distances are plotted against  $\log d/n$ . This observation is consistent with the results presented in Theorem ??, which suggests that the effective sample size is  $n/\log d$  when controlling the prediction accuracy of the eigenvectors. This finding highlights the importance of considering the relationship between  $n$  and  $d$  when evaluating the performance of SSPCA. Specifically, it suggests that as the dimension  $d$  increases, the sample size  $n$  must also increase in order to maintain a given level of prediction accuracy.

To demonstrate the computational efficiency of our proposed SSPCA method, we conducted experiments with  $d = 100$  and varying sample sizes. The results, presented in Figure 3, show the average computation time for both SSPCA and the existing method, ECA. Our findings indicate that the average computation time of SSPCA grows linearly with the sample size, whereas the computation time of ECA grows quadratically with the sample size. This observation highlights a significant advantage of SSPCA, particularly when dealing with large sample sizes. The linear growth in computation time suggests that SSPCA is able to efficiently handle increasing amounts of data, making it a preferable choice for large-scale datasets. In contrast, the quadratic growth of ECA’s computation time indicates that it may become impractical for large sample sizes due to the significantly increased computational burden. Therefore, our proposed SSPCA method offers a computationally efficient solution for analyzing large datasets, making it a valuable tool for researchers and practitioners working with big data.

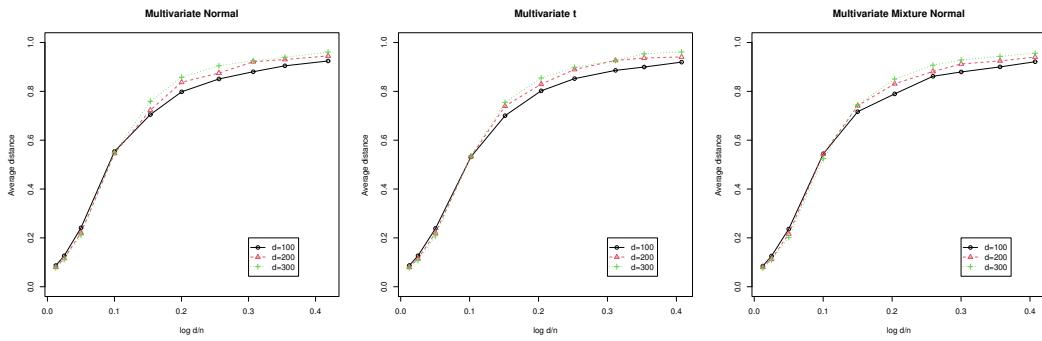
Next, we evaluate the estimation accuracy of the number of selected features. Table 1 reports the average distances between the estimates and true parameters of the leading eigenvector, comparing the estimated number of selected features  $\hat{s}$  with the true number of selected features  $s$ . We observe that the average distance with the estimated  $\hat{s}$  is slightly larger than the oracle estimator with the true  $s$ . As the sample size increases, the estimation of  $s$  improves, leading to a smaller average distance  $|\sin \angle(\hat{\mathbf{v}}_1, \mathbf{v}_1)|$  between  $\hat{s}$  and  $s$ . Figure 4 shows the histogram of the estimated number of selected features with  $n = 400$  and  $d = 300$ . Our findings indicate that both ECA and SSPCA consistently estimate the number

Figure 2: Curves of averaged distances between the estimates and true parameters with varying number of dimensions and sample size.

(a)  $s = 5$



(b)  $s = 10$



(c)  $s = 20$

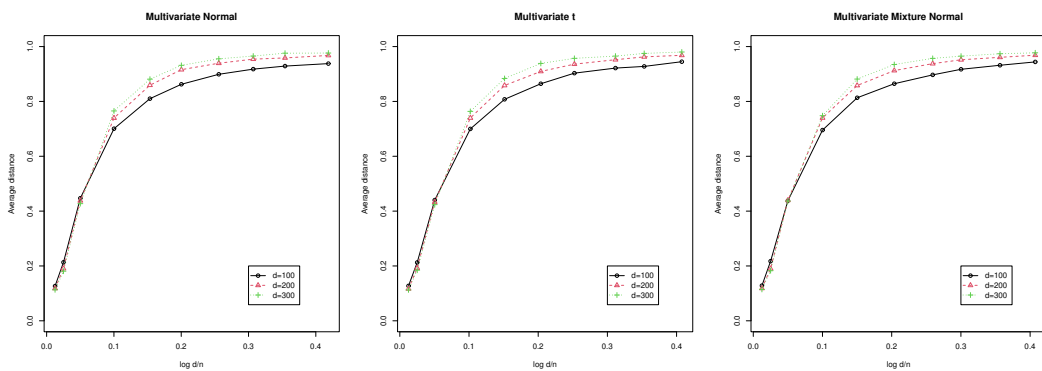
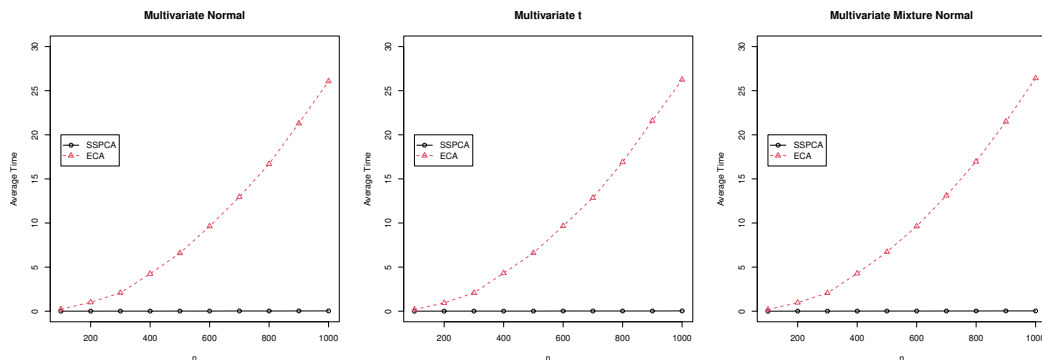


Figure 3: Average computation time of SSPCA and ECA with  $d = 100$  and varying sample sizes.



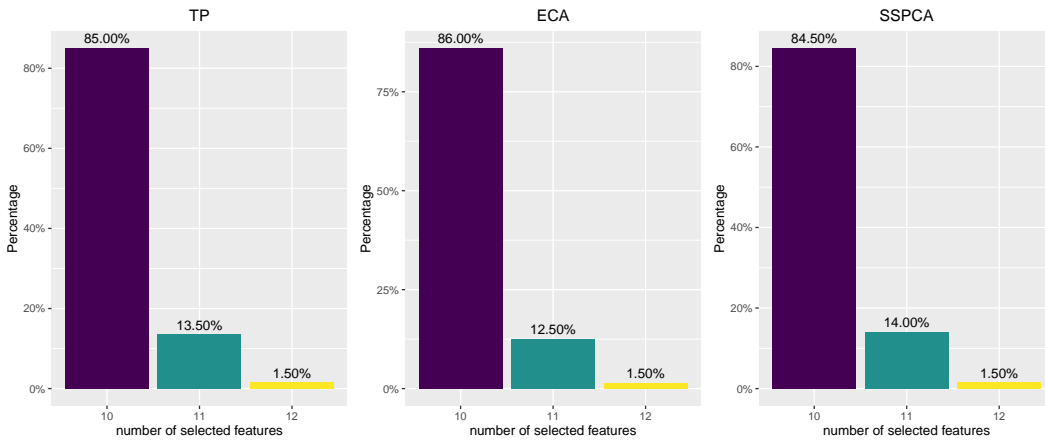
of selected features, whereas TP does not perform well with heavy-tailed distributions.

Table 1: The averaged distances between the estimates and true parameters of the leading eigenvector with estimated number of selected features  $\hat{s}$  and the true number of selected features  $s$ .

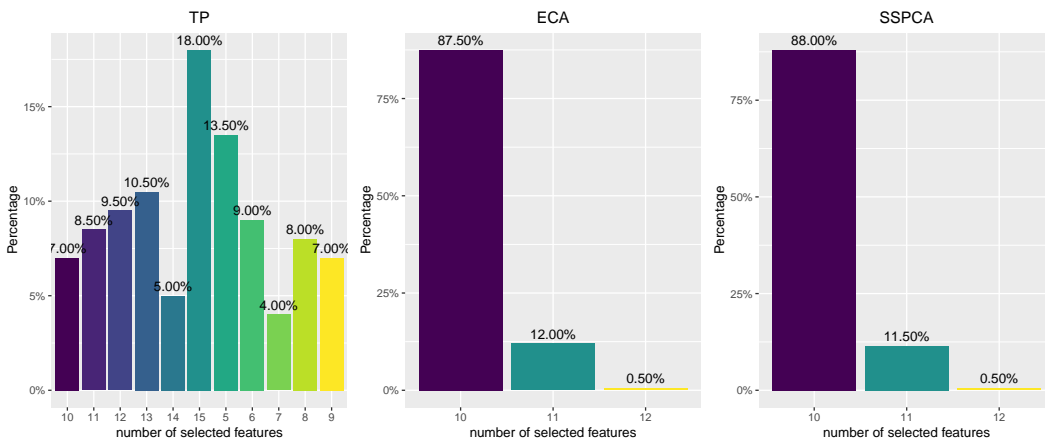
$T$	$n = 200$						$n = 400$					
	(I)		(II)		(III)		(I)		(II)		(III)	
Distributions	$\hat{s}$	$s$	$\hat{s}$	$s$	$\hat{s}$	$s$	$\hat{s}$	$s$	$\hat{s}$	$s$	$\hat{s}$	$s$
	$d = 100$											
TP	0.138	0.118	0.891	0.886	0.365	0.314	0.091	0.082	0.821	0.812	0.181	0.139
ECA	0.139	0.118	0.169	0.133	0.163	0.135	0.091	0.083	0.096	0.088	0.095	0.087
SSPCA	0.141	0.121	0.140	0.119	0.148	0.125	0.091	0.083	0.090	0.082	0.094	0.085
	$d = 200$											
TP	0.141	0.113	0.938	0.936	0.441	0.401	0.091	0.083	0.923	0.917	0.208	0.146
ECA	0.137	0.115	0.170	0.127	0.169	0.126	0.089	0.082	0.093	0.085	0.090	0.086
SSPCA	0.141	0.115	0.139	0.117	0.141	0.116	0.087	0.081	0.088	0.080	0.086	0.081
	$d = 300$											
TP	0.142	0.117	0.973	0.977	0.483	0.452	0.087	0.081	0.967	0.967	0.218	0.163
ECA	0.142	0.117	0.185	0.132	0.192	0.134	0.086	0.081	0.095	0.090	0.094	0.087
SSPCA	0.142	0.118	0.145	0.118	0.150	0.120	0.087	0.081	0.089	0.084	0.088	0.083

Figure 4: Histogram of estimator of the number of selected features with  $n = 400, d = 300$ .

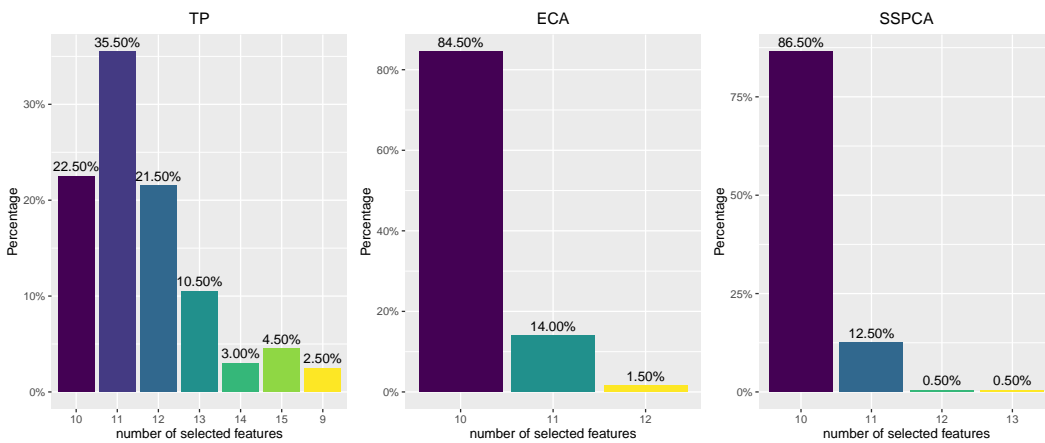
(a) Multivariate Normal



(b) Multivariate t



(c) Multivariate Mixture Normal



## 4.2 Estimating Top $m$ Leading Eigenvector

Next, we consider estimating the top  $m$  leading eigenvectors of the covariance matrix  $\Sigma$ . Here we set  $m = 4$ , the eigenvalues  $\omega_1 = 10.1, \omega_2 = 6.2, \omega_3 = 3.3, \omega_4 = 1.4, \omega_5 = \dots = \omega_d = 0.5$  and the cardinalities  $s_1 = s_2 = 10, s_3 = s_4 = 8$ . Figure 5 plots the average distances  $\frac{1}{4} \sum_{i=1}^4 |\sin \angle(\hat{\mathbf{v}}_i, \mathbf{v}_i)|$  against the numbers of estimated nonzero entries  $\frac{1}{4} \sum_{j=1}^4 \|\hat{\mathbf{v}}_j\|_0$  with  $n = 50, 100, 200$  and  $d = 100$ . For simplicity, here we set  $\|\hat{\mathbf{v}}_j\|_0$  are all equal. Our findings indicate that as the sample size increases, the estimating errors become smaller, which aligns with the results presented in Figure 2. This observation suggests that the accuracy of our estimations improves with larger sample sizes. Furthermore, similar to the results observed in Figure 1, our proposed SSPCA method consistently outperforms the other two methods when dealing with heavy-tailed distributions. This indicates that our SSPCA method is particularly effective in handling data with heavy-tailed distributions, which are common in many real-world datasets.

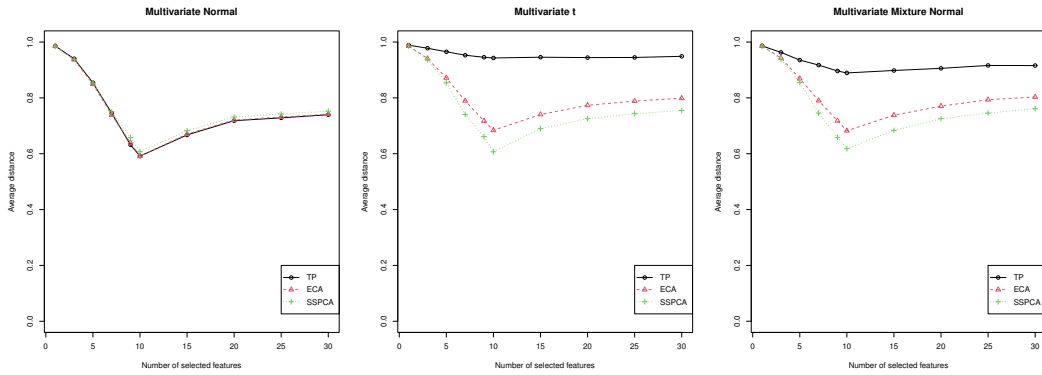
In addition, under normal distribution, our proposed SSPCA method performs similarly to the TP method. This is an important finding because it suggests that our SSPCA method can achieve comparable performance to existing methods in standard scenarios, while also demonstrating superior performance in more challenging scenarios with heavy-tailed distributions.

Next, we further investigate the impact of estimating the number of selected features on the accuracy of the average distances. In this analysis, we select  $\|\hat{\mathbf{v}}_1\|_0$  as a representative and set all other values equal to it. Table 2 reports the averaged distances between the estimates and true parameters of the top  $m$  leading eigenvectors, comparing the estimated number of selected features  $\hat{s}$  with the true number of selected features  $s$ . Figure 6 presents the histogram of the estimated number of selected features with  $n = 400$  and  $d = 100$ . The results obtained are consistent with those from the previous subsection. Specifically, the average distance with the estimated  $\hat{s}$  is slightly larger than the oracle estimator with the true  $s$ .

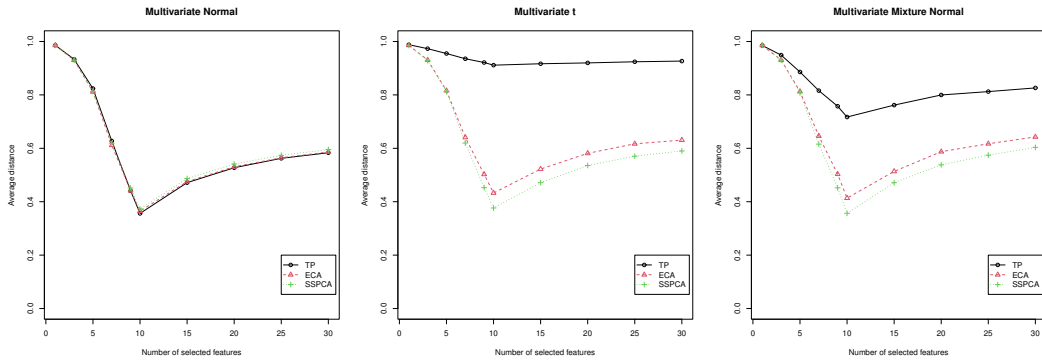
Overall, these results demonstrate the robustness and effectiveness of our proposed

Figure 5: Curves of averaged distances between the estimates and true parameters with different number of selected features on estimating top  $m$  leading eigenvectors.

(a)  $n = 50, p = 100$



(b)  $n = 100, p = 100$



(c)  $n = 200, p = 100$

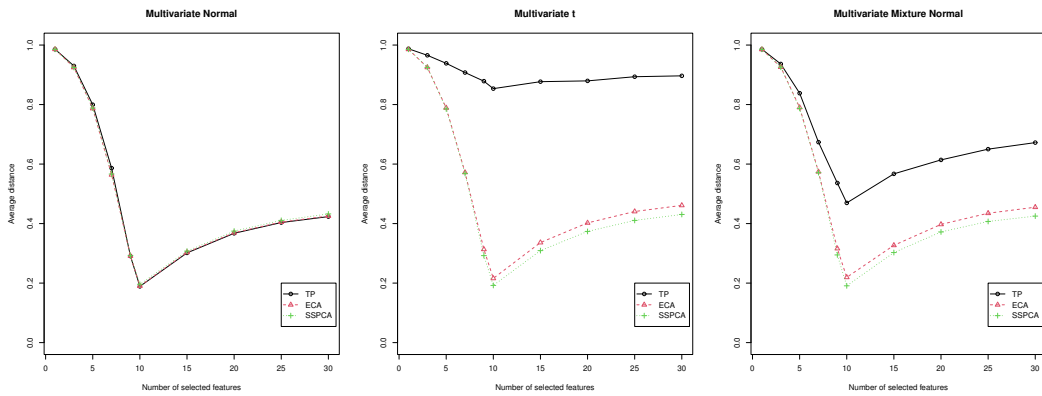
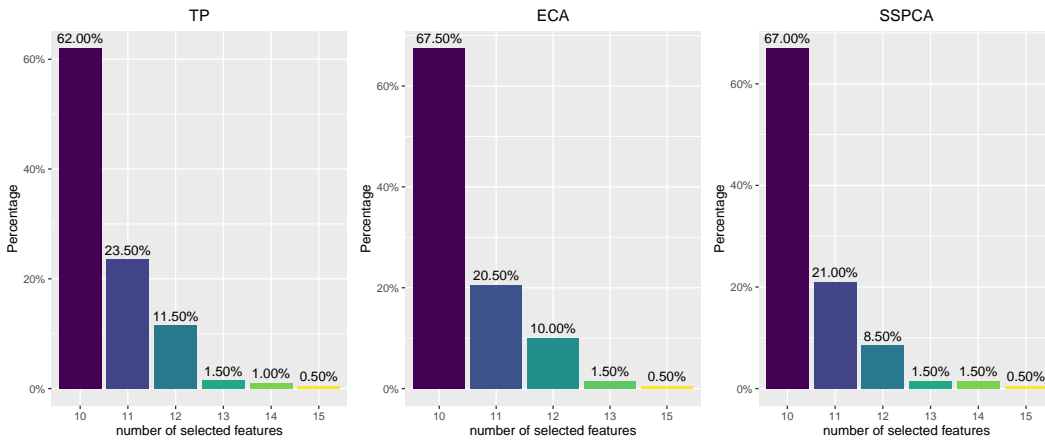
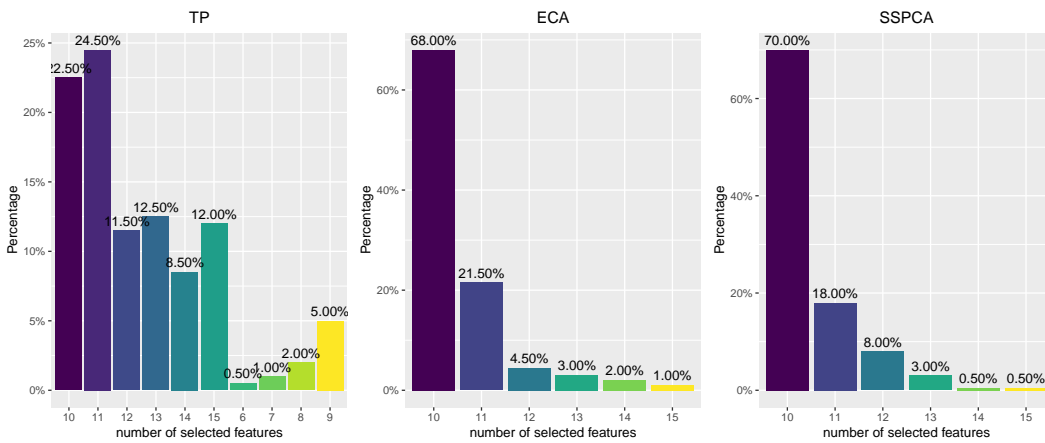


Figure 6: Histogram of estimator of the number of selected features with  $n = 400, d = 100$ .

(a) Multivariate Normal



(b) Multivariate t



(c) Multivariate Mixture Normal

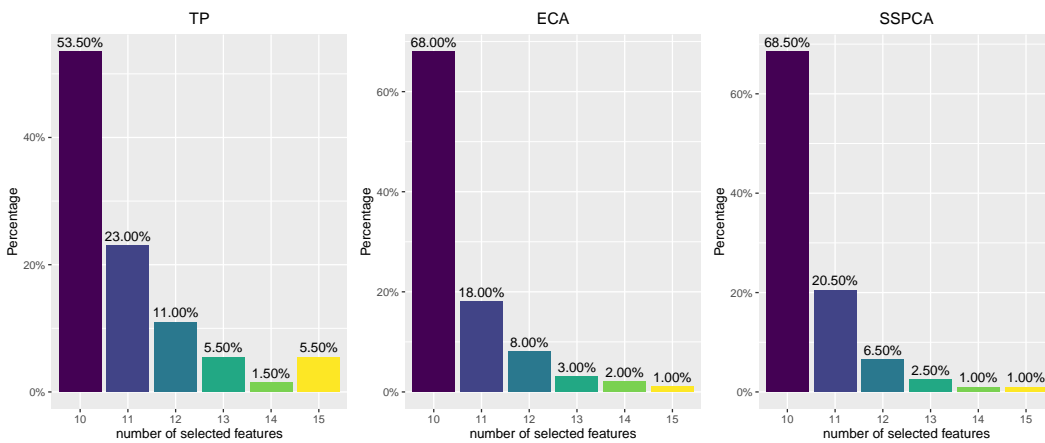




Table 2: The averaged distances between the estimates and true parameters of the top  $m$  leading eigenvector with estimated number of selected features  $\hat{s}$  and the true number of selected features  $s$ .

$T$	$n = 200$						$n = 400$					
	(I)		(II)		(III)		(I)		(II)		(III)	
Distributions	$\hat{s}$	$s$	$\hat{s}$	$s$	$\hat{s}$	$s$	$\hat{s}$	$s$	$\hat{s}$	$s$	$\hat{s}$	$s$
	$d = 100$											
TP	0.184	0.168	0.859	0.847	0.483	0.446	0.128	0.115	0.790	0.767	0.268	0.237
ECA	0.188	0.176	0.245	0.233	0.236	0.217	0.127	0.116	0.136	0.123	0.140	0.127
SSPCA	0.195	0.182	0.216	0.204	0.209	0.196	0.130	0.120	0.131	0.121	0.128	0.117

SSPCA method in handling various types of data distributions. The ability to accurately estimate parameters even in the presence of heavy-tailed distribution is a valuable characteristic of our method, and it highlights its potential for use in a wide range of applications where data may not always follow a normal distribution.

## 5 Real Data Analysis

In this section, we apply three methodologies—Thresholding Pursuit (TP), Exponential Component Analysis (ECA), and Sparse and Structured Principal Component Analysis (SSPCA)—to analyze the Standard & Poor’s 500 (S&P 500) index. To account for the dynamic nature of the index’s composition over time, we compiled monthly returns for all securities included in the S&P 500 from January 2005 to November 2018 ( $n = 165$ ). Given the evolving nature of the index, we focused on a consistent subset of  $d = 374$  securities that were present throughout this entire period. As demonstrated in Liu et al. (2023), stock returns exhibit non-Gaussian, heavy-tailed characteristics, which necessitate the use of robust statistical procedures. For simplicity, our analysis considers only the first two principal components.

Utilizing a tuning parameter selection procedure, we determined optimal values of  $k = d$  for the first principal component and  $k = 150$  for the second principal component. Figure 7 displays scatter plots of the first principal component (PC1) versus the second principal component (PC2) for each of the three methodologies—TP, ECA, and SSPCA.

Consistent with the approach in Han and Liu (2018), red dots in the plots represent potential outliers with strong leverage influence. Leverage strength, defined as the diagonal values of the hat matrix in a linear regression model where the first principal component is regressed on the second, serves as an indicator of the impact of individual data points on the regression estimates (Neter et al., 1996). High leverage strength implies that the inclusion of these points will significantly affect the linear regression estimates applied to the principal components of the data. We chose a threshold value of 0.05 to identify data points with strong leverage influence. Our analysis revealed that 6 data points have strong leverage influence for the TP method, 2 for the ECA method, and only 1 for the SSPCA method. These findings highlight the robustness of our proposed SSPCA method.

Furthermore, we examined the leverage influence of each data point over time for each methodology, as depicted in Figure 8. We observed that data points with strong leverage influence tend to cluster around periods of financial crisis, indicating that these observations could have a profound impact on statistical inference. Notably, our SSPCA method exhibits reduced sensitivity to these outliers compared to the other methodologies. This robustness is particularly advantageous in financial applications, where outliers and extreme events are common and can significantly affect analysis results.

## 6 Conclusion

In this paper, we analyze the application of principal component analysis (PCA) with a sample spatial-sign covariance matrix in high-dimensional contexts. We determine the approximation errors of the principal component estimator under both non-sparse and sparse conditions. Simulation studies and real-world data applications demonstrate the computa-

Figure 7: Plots of principal components 1 (PC1) against principal components 2 (PC2) with three methods—TP, ECA and SSPCA. Here red dots represent the points with strong leverage influence.

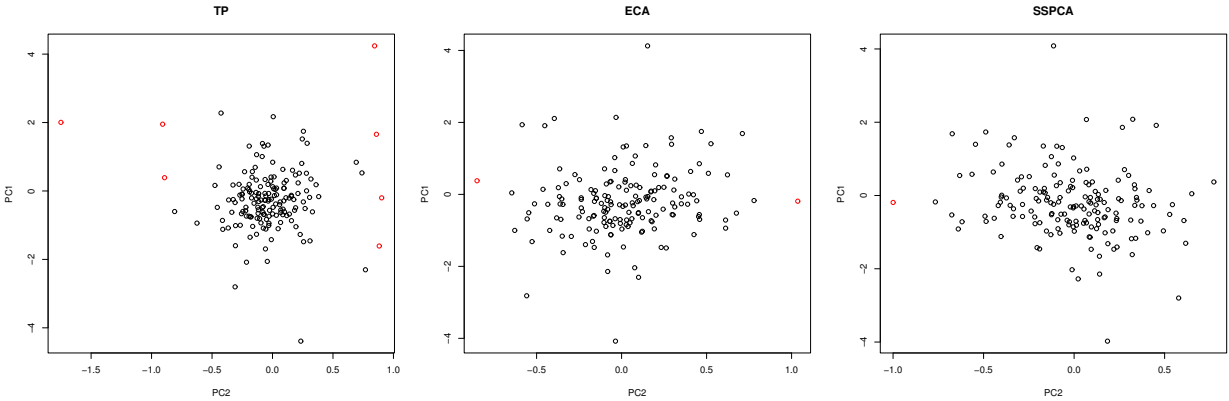
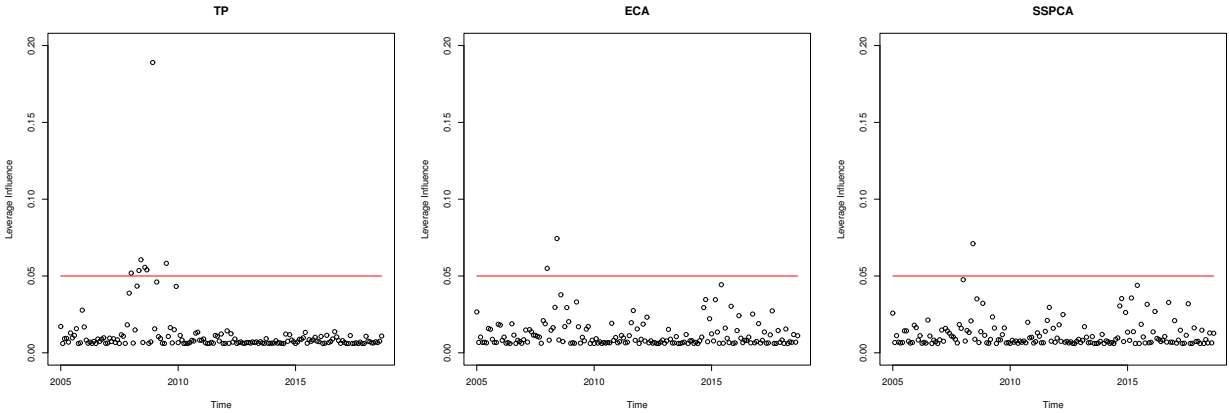


Figure 8: Leverage influence of each method over time period.



tional efficiency and robustness of our proposed methods. PCA is a widely utilized technique in numerous fields, and therefore, the methods presented in this paper can be applied to various applications, including high-dimensional factor analysis (He et al., 2022) and dimension reduction (Chen et al., 2022).

## 7 Appendix

### 7.1 Appendix A: Fantope Projection

Similar to Vu et al. (2013), we define  $\mathbf{Y}_1$  as the solution to the following convex program:

$$\mathbf{Y}_1 := \arg \max_{\mathbf{M} \in \mathbb{R}^{d \times d}} \langle \widehat{\mathbf{S}}, \mathbf{M} \rangle - \lambda \sum_{j,k} |\mathbf{M}_{jk}|, \text{ subject to } \mathbf{0} \preceq \mathbf{M} \preceq \mathbf{I}_d \text{ and } \text{Tr}(\mathbf{M}) = 1,$$

where for any two matrices  $\mathbf{A}, \mathbf{B} \in \mathbb{R}^{d \times d}$ ,  $\mathbf{A} \preceq \mathbf{B}$  represents that  $\mathbf{B} - \mathbf{A}$  is positive semidefinite. Here,  $\{\mathbf{M} : \mathbf{0} \preceq \mathbf{M} \preceq \mathbf{I}_d, \text{Tr}(\mathbf{M}) = 1\}$  is a convex set called the Fantope. The initial parameter  $\mathbf{v}^{(0)}$  then, is the normalized vector consisting of the largest entries in  $\mathbf{u}_1(\mathbf{Y}_1)$ , where  $\mathbf{Y}_1$  is calculated in (5.1):

$$\mathbf{v}^{(0)} = \mathbf{w}^0 / \|\mathbf{w}^0\|_2, \text{ where } \mathbf{w}^0 = \text{TRC}(\mathbf{u}_1(\mathbf{Y}_1), J_\varphi) \text{ and } J_\varphi = \left\{ j : \left| (\mathbf{u}_1(\mathbf{Y}_1))_j \right| \geq \varphi \right\} \quad (9)$$

We have  $\|\mathbf{v}^{(0)}\|_0 = \text{supp} \left\{ j : \left| (\mathbf{u}_1(\mathbf{Y}_1))_j \right| > 0 \right\}$ . To show the consistency of the initial estimator, we need the following assumptions:

(C1)  $\text{rank}(\boldsymbol{\Sigma}) = q$  and  $\|\mathbf{u}_1(\boldsymbol{\Sigma})\|_0 \leq s$ . Additionally, we assume  $\nu_i$  is sub-gaussian distributed, i.e.  $\|\nu_i\|_{\psi_2} \leq K_\nu < \infty$ .

(C2)  $\lambda_1(\boldsymbol{\Sigma})/q\lambda_q(\boldsymbol{\Sigma}) = O(\lambda_1(\mathbf{K}))$ ,  $\|\boldsymbol{\Sigma}\|_{\text{F}} \log d = o(\text{Tr}(\boldsymbol{\Sigma}))$ .  $\lambda_2(\boldsymbol{\Sigma})/\lambda_1(\boldsymbol{\Sigma})$  is upper bounded by an absolute constant less than 1, and  $\lambda \asymp \lambda_1(\mathbf{K})\sqrt{\log d/n}$ .

(C3) let  $J_0 := \left\{ j : \left| (\mathbf{u}_1(\mathbf{K}))_j \right| = \Omega^0(s \log d/\sqrt{n}) \right\}$ . Set  $\varphi$  in (9) to be  $\varphi = C_2 s(\log d)/\sqrt{n}$  for some positive absolute constant  $C_2$ . If  $s\sqrt{\log d/n} \rightarrow 0$ , and  $\|(\mathbf{u}_1(\mathbf{K}))_{J_0}\|_2 \geq C_3 > 0$  is lower bounded by an absolute positive constant.

**THEOREM 7.1** *Under Assumption (A1)-(A2) and (C1), if  $(\log d + \log(1/\alpha))/n \rightarrow 0$  and  $\lambda \geq C_1 \left( \frac{8\lambda_1(\Sigma)}{q\lambda_q(\Sigma)} + \|\mathbf{S}\|_{\max} \right) \sqrt{\frac{\log d + \log(1/\alpha)}{n}}$ , for sufficient large  $n$ , we have*

$$|\sin \angle(\mathbf{u}_1(\mathbf{Y}_1), \mathbf{u}_1(\mathbf{S}))| \leq \frac{8\sqrt{2}s\lambda}{\lambda_1(\mathbf{S}) - \lambda_2(\mathbf{K})},$$

*with probability larger than  $1 - \alpha^2$ . Additionally, if condition (C2) also hold, we have*

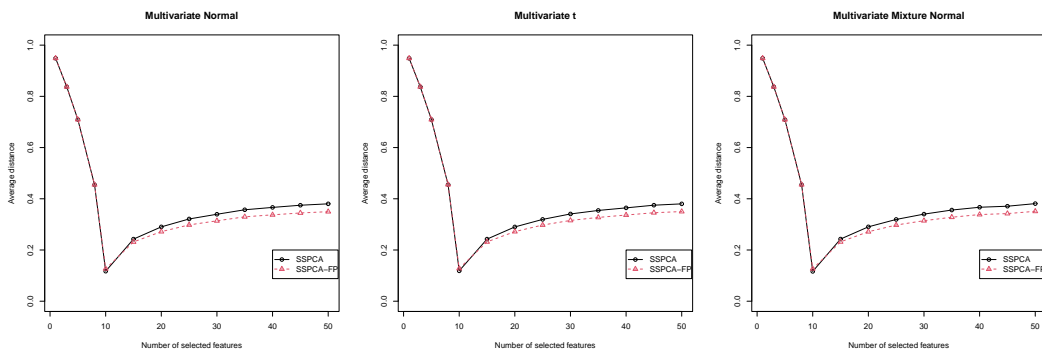
$$|\sin \angle(\mathbf{u}_1(\mathbf{Y}_1), \mathbf{u}_1(\mathbf{S}))| = O_p \left( s \sqrt{\frac{\log d}{n}} \right).$$

*Then, if condition (C3) also hold, with probability tending to 1,  $\|\mathbf{v}^{(0)}\|_0 \leq s$  and  $\left| (\mathbf{v}^{(0)})^T \mathbf{u}_1(\mathbf{S}) \right|$  is lower bounded by  $C_3/2$ .*

Next, we conduct simulation studies to compare the two distinct initial estimators. SSPCA denotes the proposed method utilizing the eigenvector as the initial estimator, whereas SSPCA-FP refers to the proposed method incorporating Fantope Projection. In this analysis, we focus solely on the estimation of the first eigenvector. Figure 9 presents the outcomes of these two approaches. Our observations reveal that when the number of selected features matches the true number, SSPCA-FP performs similar to SSPCA. However, when the number of selected features exceeds the true parameters, SSPCA-FP exhibits smaller averaged distances compared to SSPCA. We also compare these two methods with the averaged distances between the estimates and true parameters of the leading eigenvector with estimated number of selected features  $\hat{s}$ . Table 3 reveals the simulation results with the same settings as Table 1. Overall, the performance of these two initial estimators is quite comparable. SSPCA-FP exhibits slightly smaller averaged distances when compared to the estimator  $\hat{s}$ . Therefore, if computational time is not a constraint, we recommend using SSPCA-FP as the primary choice.

Figure 9: Curves of averaged distances between the estimates and true parameters with different number of selected features on estimating leading eigenvectors.

(a)  $n = 200, d = 100$



(b)  $n = 200, d = 200$

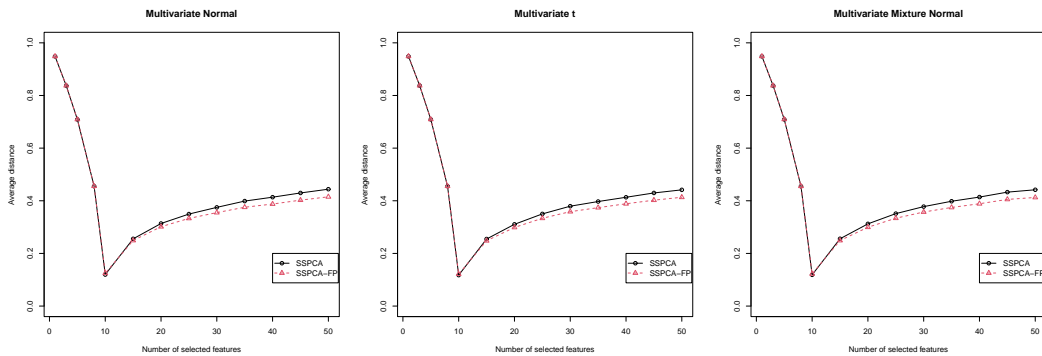


Table 3: The averaged distances between the estimates and true parameters of the leading eigenvector with estimated number of selected features  $\hat{s}$  and the true number of selected features  $s$ .

$T$	$n = 200$						$n = 400$					
	(I)		(II)		(III)		(I)		(II)		(III)	
Distributions	$\hat{s}$	$s$	$\hat{s}$	$s$	$\hat{s}$	$s$	$\hat{s}$	$s$	$\hat{s}$	$s$	$\hat{s}$	$s$
	$d = 100$											
SSPCA	0.141	0.121	0.140	0.119	0.148	0.125	0.091	0.083	0.090	0.082	0.094	0.085
SSPCA-FP	0.140	0.125	0.143	0.129	0.145	0.126	0.090	0.085	0.091	0.081	0.093	0.085
	$d = 200$											
SSPCA	0.141	0.115	0.139	0.117	0.141	0.116	0.087	0.081	0.088	0.080	0.086	0.081
SSPCA-FP	0.142	0.116	0.138	0.117	0.140	0.119	0.086	0.083	0.087	0.082	0.086	0.082
	$d = 300$											
SSPCA	0.142	0.118	0.145	0.118	0.150	0.120	0.087	0.081	0.089	0.084	0.088	0.083
SSPCA-FP	0.141	0.120	0.139	0.120	0.141	0.117	0.086	0.083	0.087	0.085	0.086	0.083

## 7.2 Appendix B: Proof of Theorems

### 7.2.1 Some useful lemmas

The accuracies of constant and linear approximations of function  $|\mathbf{y} - \mu|^{-1}(\mathbf{y} - \mu)$  of  $\mu$  are given by 1 .

**LEMMA 7.1** *Let  $\mathbf{y} \neq \mathbf{0}$  and  $\mu$  be any  $p$ -vectors,  $p > 1$ . Write also  $r = |\mathbf{y}|$  and  $\mathbf{u} = |\mathbf{y}|^{-1}\mathbf{y}$ .*

$$\left| \frac{\mathbf{y} - \mu}{|\mathbf{y} - \mu|} - \frac{\mathbf{y}}{|\mathbf{y}|} \right| \leq 2 \frac{|\mu|}{r}$$

$$\left| \frac{\mathbf{y} - \mu}{|\mathbf{y} - \mu|} - \frac{\mathbf{y}}{|\mathbf{y}|} - \frac{1}{r} [\mathbf{I}_p - \mathbf{u}\mathbf{u}'] \mu \right| \leq C \frac{|\mu|^{1+\delta}}{r^{1+\delta}}$$

for all  $0 < \delta < 1$  where  $C$  does not depend on  $\mathbf{y}$  or  $\mu$ .

The following lemma is the result of the Lemma 19 of Arcones (1998). See also Bai et al. (1990) and Oja (2010).

**LEMMA 7.2** *The accuracies of constant, linear and quadratic approximations of the function  $\boldsymbol{\mu} \mapsto \|\mathbf{z} - \boldsymbol{\mu}\|$  can be given by*

$$(1) \quad \left| \|\mathbf{z} - \boldsymbol{\mu}\| - \|\mathbf{z}\| \right| \leq \|\boldsymbol{\mu}\|,$$

$$(2) \quad \left| \|\mathbf{z} - \boldsymbol{\mu}\| - \|\mathbf{z}\| + \mathbf{u}^T \boldsymbol{\mu} \right| \leq 2r^{-1} \|\boldsymbol{\mu}\|^2,$$

$$(3) \quad \left| \|\mathbf{z} - \boldsymbol{\mu}\| - \|\mathbf{z}\| + \mathbf{u}^T \boldsymbol{\mu} - \boldsymbol{\mu}^T (2r)^{-1} [\mathbf{I}_p - \mathbf{u}\mathbf{u}^T] \boldsymbol{\mu} \right| \leq cr^{-1-\delta} \|\boldsymbol{\mu}\|^{2+\delta} \text{ for all } 0 < \delta < 1,$$

where  $\mathbf{z} = r\mathbf{u}$ ,  $r = \|\mathbf{z}\|$ ,  $\mathbf{u} = \|\mathbf{z}\|^{-1}\mathbf{z}$  and the constant  $c$  does not depend on  $\mathbf{z}$  or  $\boldsymbol{\mu}$ .

Next, we restate Theorem 1.4 in Tropp (2012).

**LEMMA 7.3** *(Matrix Bernstein) Consider a finite sequence  $\{\mathbf{X}_k\}$  of independent, random, self-adjoint matrices with dimension  $d$ . Assume that each random matrix satisfies*

$$E\mathbf{X}_k = \mathbf{0} \quad \text{and} \quad \lambda_{\max}(\mathbf{X}_k) \leq R \quad \text{almost surely}$$

Then, for all  $t \geq 0$ ,

$$P \left\{ \left\| \sum_k \mathbf{X}_k \right\|_2 \geq t \right\} \leq d \cdot \exp \left( \frac{-t^2/2}{\sigma^2 + Rt/3} \right) \quad \text{where } \sigma^2 := \left\| \sum_k E(\mathbf{X}_k^2) \right\|_2.$$

**LEMMA 7.4** *Under conditions (A1)-(A2), we have  $\hat{\boldsymbol{\mu}} - \boldsymbol{\mu} = O_p(\zeta_1^{-1}n^{-1/2})$  and*

$$\hat{\boldsymbol{\mu}} - \boldsymbol{\mu} = \zeta_1^{-1} \frac{1}{n} \sum_{i=1}^n \mathbf{U}_i + o_p(\zeta_1^{-1}n^{-1/2}).$$

**Proof:** Define the object function

$$L(\boldsymbol{\theta}) = \sum_{i=1}^n \|\mathbf{X}_i - \boldsymbol{\mu} - \boldsymbol{\theta}\| - \sum_{i=1}^n \|\mathbf{X}_i - \boldsymbol{\mu}\|$$

and  $\hat{\boldsymbol{\theta}} = \arg \max L(\boldsymbol{\theta})$ . Then  $\hat{\boldsymbol{\theta}} = \hat{\boldsymbol{\mu}} - \boldsymbol{\mu}$ . Next, we proof that for any  $\epsilon > 0$ , there exists  $C > 0$  such that

$$\liminf_n P \left( \inf_{\mathbf{u} \in \mathbb{S}^{d-1}} L(C\zeta_1^{-1}n^{-1/2}\mathbf{u}) > 0 \right) \geq 1 - \epsilon$$



for large enough  $n$ . Then, by the convexity of  $L(\cdot)$ , we can obtain

$$P\left(\|\hat{\boldsymbol{\theta}}\| \leq C\zeta_1^{-1}n^{-1/2}\right) \geq 1 - \epsilon,$$

which means  $\hat{\boldsymbol{\theta}} = O_p(\zeta_1^{-1}n^{-1/2})$ . By Lemma 7.2, we have

$$\begin{aligned} L(C\zeta_1^{-1}n^{-1/2}\mathbf{u}) &\geq -C\sum_{i=1}^n(\zeta_1^{-1}n^{-1/2}\mathbf{U}_i^T\mathbf{u}) \\ &\quad + C^2\sum_{i=1}^n\zeta_1^{-2}n^{-1}\frac{1}{2r_i}\mathbf{u}^T[\mathbf{I}_d - \mathbf{U}_i\mathbf{U}_i^T]\mathbf{u} \\ &\quad - \sum_{i=1}^n cC^{2+\delta}\frac{1}{r_i^{1+\delta}}\zeta_1^{-(2+\delta)}n^{-1-\frac{1}{2}\delta} \\ &\doteq A_1 + A_2 + A_3. \end{aligned}$$

Because  $(\mathbf{U}_i^T\mathbf{u})^2 \leq 1$ ,  $E(\mathbf{U}_i^T\mathbf{u}) = 0$  and  $\text{Var}(\mathbf{U}_i^T\mathbf{u}) = \mathbf{u}^T\mathbf{S}\mathbf{u} \leq \|\mathbf{S}\|_2 \leq \text{tr}(\mathbf{S}) = 1$ , so, by Chebyshev inequality, for sufficient large  $M > 0$ , we have

$$P\left(\sum_{i=1}^n n^{-1/2}\mathbf{U}_i^T\mathbf{u} > M\right) \leq \frac{1}{M} \leq \frac{\epsilon}{3}.$$

Thus, with at least probability  $1 - \frac{\epsilon}{3}$ , we have

$$-C\sum_{i=1}^n(\zeta_1^{-1}n^{-1/2}\mathbf{U}_i^T\mathbf{u}) \geq -C\zeta_1^{-1}M.$$

In addition,  $E(1 - (\mathbf{U}_i^T\mathbf{u})^2) = 1 - \mathbf{u}^T\mathbf{S}\mathbf{u} \geq 1 - \|\mathbf{S}\|_2 > \varphi > 0$  by condition (A1),  $\text{Var}(\zeta_1^{-1}r_i^{-1}[1 - (\mathbf{U}_i^T\mathbf{u})^2]) \leq E(\zeta_1^{-2}r_i^{-2})E((\mathbf{U}_i\mathbf{u})^4) - (\mathbf{u}^T\mathbf{S}\mathbf{u})^2 \leq \zeta_1^{-2}\zeta_2 \leq \zeta$ . Thus, by Chebyshev inequality, we have

$$\begin{aligned} &P\left(\frac{1}{n}\sum_{i=1}^n\zeta_1^{-1}\frac{1 - (\mathbf{U}_i^T\mathbf{u})^2}{2r_i} - \frac{1}{2}(1 - \mathbf{u}^T\mathbf{S}\mathbf{u}) \leq -\frac{1}{4}(1 - \mathbf{u}^T\mathbf{S}\mathbf{u})\right) \\ &\leq \frac{4\text{Var}(\zeta_1^{-1}r_i^{-1}[1 - (\mathbf{U}_i^T\mathbf{u})^2])}{n(1 - \mathbf{u}^T\mathbf{S}\mathbf{u})} \leq \frac{4\zeta}{n\psi} \leq \frac{\epsilon}{3} \end{aligned}$$

for sufficient large  $n$ . Thus, with at least probability  $1 - \frac{\epsilon}{3}$ , we have

$$A_2 \geq \frac{C^2}{4\zeta_1}(1 - \mathbf{u}^T\mathbf{S}\mathbf{u}) \geq \frac{C^2\psi}{4\zeta_1}.$$

Finally, by the Chebyshev inequality, we have

$$P\left(\frac{1}{n}\sum_{i=1}^n\frac{1}{r_i^{1+\delta}}\zeta_1^{-(1+\delta)}\geq\frac{1}{2}E(\nu_i^{1+\delta})\right)\leq\frac{4\text{Var}(\nu_i^{1+\delta})}{n[E(\nu_i^{1+\delta})]^2}\leq\frac{4\zeta}{n}\leq\frac{\epsilon}{3}$$

by condition (A1) for sufficient large  $n$ . So  $A_3\geq\frac{cC^{2+\delta}}{2\zeta_1}E(\nu_i^{1+\delta})n^{-\frac{1}{2}\delta}$ . Thus, at least probability  $1-\epsilon$ , we have

$$\zeta_1L(\zeta_1^{-1}n^{-1/2+\epsilon}\mathbf{u})\geq-CM+\frac{C^2\psi}{4}-\frac{cC^{2+\delta}}{2}E(\nu_i^{1+\delta})n^{-\frac{1}{2}\delta}>0$$

for large enough  $n$  and  $C$ .

Next, we consider the equation  $\sum_{i=1}^nU(\mathbf{X}_i-\hat{\boldsymbol{\mu}})=0$ . Note that

$$\sum_{i=1}^nU(\mathbf{X}_i-\hat{\boldsymbol{\mu}})=\sum_{i=1}^n\frac{\mathbf{X}_i-\boldsymbol{\mu}-\hat{\boldsymbol{\theta}}}{\|\mathbf{X}_i-\boldsymbol{\mu}-\hat{\boldsymbol{\theta}}\|}=\sum_{i=1}^n\frac{\mathbf{U}_i-r_i^{-1}\hat{\boldsymbol{\theta}}}{(1+2r_i^{-1}\mathbf{U}_i^T\hat{\boldsymbol{\theta}}+r_i^{-2}\|\hat{\boldsymbol{\theta}}\|_2^2)^{1/2}}$$

which implies that

$$\left\{n^{-1}\sum_{i=1}^nr_i^{-1}+O_p(\zeta_1n^{-1/2})\right\}\hat{\boldsymbol{\theta}}-\left\{n^{-1}\sum_{i=1}^nr_i^{-1}\mathbf{U}_i\mathbf{U}_i^T\right\}\hat{\boldsymbol{\theta}}=\left(n^{-1}\sum_{i=1}^n\mathbf{U}_i\right)(1+O_p(n^{-1})).$$

Then, we obtained that

$$\hat{\boldsymbol{\theta}}=(\zeta_1+O_p(\zeta_1n^{-1/2}))^{-1}\left(n^{-1}\sum_{i=1}^n\mathbf{U}_i\right)\{1+O_p(n^{-1})\}=n^{-1}\zeta_1^{-1}\sum_{i=1}^n\mathbf{U}_i+O_p(\zeta_1^{-1}n^{-1})$$

### 7.2.2 Proof of Theorem 2.1

Define  $\tilde{\mathbf{S}}=\frac{1}{n}\sum_{i=1}^n\mathbf{U}_i\mathbf{U}_i^T$ ,  $\mathbf{U}_i=U(\mathbf{X}_i-\boldsymbol{\mu})$ . Obviously,

$$\|\mathbf{U}_i\mathbf{U}_i^T-\mathbf{S}\|_2\leq\|\mathbf{U}_i\mathbf{U}_i^T\|_2+\|\mathbf{S}\|_2=1+\|\mathbf{S}\|_2,$$

and

$$\|E[(\mathbf{U}_i\mathbf{U}_i^T-\mathbf{S})^2]\|_2=\|\mathbf{S}-\mathbf{S}^2\|_2\leq\|\mathbf{S}\|_2+\|\mathbf{S}\|_2^2.$$

Thus, according to Lemma 7.3, we have

$$\begin{aligned}P\left(\|\tilde{\mathbf{S}}-\mathbf{S}\|_2\geq t\right)&\leq d\cdot\exp\left(\frac{-nt^2/2}{(\|\mathbf{S}\|_2+\|\mathbf{S}\|_2^2)+(1+\|\mathbf{S}\|_2)t/3}\right)\\&\leq d\cdot\exp\left(\frac{-nt^2}{4(\|\mathbf{S}\|_2+\|\mathbf{S}\|_2^2)}\right)\end{aligned}$$

for small enough  $t \leq 3 \|\mathbf{S}\|_2$ . Setting

$$t = \sqrt{\frac{4(\|\mathbf{S}\|_2 + \|\mathbf{S}\|_2^2)(\log d + \log(3/\alpha))}{n}} = \|\mathbf{S}\|_2 \sqrt{\frac{4(1 + r^*(\mathbf{S}))(\log d + \log(3/\alpha))}{n}}$$

we have  $P\left(\|\tilde{\mathbf{S}} - \mathbf{S}\|_2 \geq t\right) \leq \alpha/3$ .

Next, we will show the bound of  $\|\hat{\mathbf{S}} - \tilde{\mathbf{S}}\|_2$ . Define  $\hat{\mathbf{U}}_i = U(\mathbf{X}_i - \hat{\boldsymbol{\mu}})$ .

$$\begin{aligned} \hat{\mathbf{S}} - \tilde{\mathbf{S}} &= \frac{1}{n} \sum_{i=1}^n [\hat{\mathbf{U}}_i \hat{\mathbf{U}}_i^T - \mathbf{U}_i \mathbf{U}_i^T] \\ &= \frac{2}{n} \sum_{i=1}^n [\hat{\mathbf{U}}_i - \mathbf{U}_i] \mathbf{U}_i^T + \frac{1}{n} \sum_{i=1}^n [\hat{\mathbf{U}}_i - \mathbf{U}_i] [\hat{\mathbf{U}}_i - \mathbf{U}_i]^T \end{aligned}$$

For any  $\mathbf{v} \in \mathbb{S}^{d-1}$ ,

$$\begin{aligned} \frac{1}{n} \sum_{i=1}^n \mathbf{v}^T [\hat{\mathbf{U}}_i - \mathbf{U}_i] [\hat{\mathbf{U}}_i - \mathbf{U}_i]^T \mathbf{v} &= \frac{1}{n} \sum_{i=1}^n ([\hat{\mathbf{U}}_i - \mathbf{U}_i]^T \mathbf{v})^2 \\ &\leq \frac{1}{n} \sum_{i=1}^n \|\hat{\mathbf{U}}_i - \mathbf{U}_i\|_2^2 \end{aligned}$$

By Lemma 7.1, we have

$$\|U(\mathbf{X}_i - \hat{\boldsymbol{\mu}}) - U(\mathbf{X}_i - \boldsymbol{\mu})\|_2 \leq 2 \frac{\|\hat{\boldsymbol{\mu}} - \boldsymbol{\mu}\|_2}{r_i}.$$

Thus,

$$\frac{1}{n} \sum_{i=1}^n \|\hat{\mathbf{U}}_i - \mathbf{U}_i\|_2^2 \leq \frac{1}{n} \sum_{i=1}^n r_i^{-2} \|\hat{\boldsymbol{\mu}} - \boldsymbol{\mu}\|_2^2.$$

By lemma 7.4, we have, there exist a positive constant  $C_\alpha$  such that  $\|\hat{\boldsymbol{\mu}} - \boldsymbol{\mu}\|_2^2 \leq C_\alpha^2 \zeta_1^{-2} n^{-1}$  with probability larger than  $1 - \alpha/6$ . Additionally, by Chebyshev inequality,

$$P\left(\frac{1}{n} \sum_{i=1}^n r_i^{-2} \zeta_1^{-2} \geq 2E(\nu_i^2)\right) \leq \frac{\kappa_\nu}{n(1 + \sigma_\nu^2)^2} \leq \frac{\alpha}{6}$$

for sufficient large  $n$ . So, with probability larger than  $1 - \frac{\alpha}{3}$ , we have

$$\left\| \frac{1}{n} \sum_{i=1}^n [\hat{\mathbf{U}}_i - \mathbf{U}_i] [\hat{\mathbf{U}}_i - \mathbf{U}_i]^T \right\|_2 \leq \frac{1}{n} \sum_{i=1}^n r_i^{-2} \|\hat{\boldsymbol{\mu}} - \boldsymbol{\mu}\|_2^2 \leq 2C_\alpha^2 \zeta n^{-1}.$$

By Lemma 7.1, we can rewrite

$$\hat{\mathbf{U}}_i - \mathbf{U}_i = r_i^{-1}[\mathbf{I}_d - \mathbf{U}_i \mathbf{U}_i^T] \hat{\boldsymbol{\theta}} + \omega_i$$

where  $\|\omega_i\|_2 \leq Cr_i^{-1-\delta} \|\hat{\boldsymbol{\theta}}\|_2^{1+\delta}$ . Thus,

$$\frac{2}{n} \sum_{i=1}^n [\hat{\mathbf{U}}_i - \mathbf{U}_i] \mathbf{U}_i^T = \frac{2}{n} \sum_{i=1}^n r_i^{-1} [\mathbf{I}_d - \mathbf{U}_i \mathbf{U}_i^T] \hat{\boldsymbol{\theta}} \mathbf{U}_i^T + \frac{2}{n} \sum_{i=1}^n \omega_i \mathbf{U}_i^T.$$

First, for any  $\mathbf{u} \in \mathbb{S}^{d-1}$ ,

$$\begin{aligned} \frac{2}{n} \sum_{i=1}^n \mathbf{u}^T \omega_i \mathbf{U}_i^T \mathbf{u} &\leq 2 \sqrt{\frac{1}{n} \sum_{i=1}^n (\mathbf{u}^T \omega_i)^2 \frac{1}{n} \sum_{i=1}^n (\mathbf{u}^T \mathbf{U}_i)^2} \\ &\leq 2 \sqrt{\frac{1}{n} \sum_{i=1}^n \|\omega_i\|_2^2} \leq 2C \|\hat{\boldsymbol{\theta}}\|_2^{1+\delta} \sqrt{\frac{1}{n} \sum_{i=1}^n r_i^{-2-2\delta}}. \end{aligned}$$

Similarly, by the Chebyshev inequality, we have

$$P \left( \frac{1}{n} \sum_{i=1}^n r_i^{-2-2\delta} \zeta_1^{-2-2\delta} \geq 2E(\nu_i^{2+2\delta}) \right) \leq \frac{\text{Var}(\nu_i^{2+2\delta})}{n[E(\nu_i^{2+2\delta})]^2} \leq \frac{\alpha}{12}$$

for sufficient large  $n$ . So, with probability larger than  $1 - \alpha/4$ , we have

$$\begin{aligned} \left\| \frac{2}{n} \sum_{i=1}^n \omega_i \mathbf{U}_i^T \right\|_2 &\leq 2\sqrt{2}C \zeta_1^{1+\delta} \|\hat{\boldsymbol{\theta}}\|_2^{1+\delta} [E(\nu_i^{2+2\delta})]^{1/2} \\ &\leq 2\sqrt{2}C C_\alpha^{1+\delta} \zeta_1^{\frac{1+\delta}{4}} n^{-\frac{1}{2}(1+\delta)}. \end{aligned}$$

By Lemma 7.4, we can write  $\hat{\boldsymbol{\theta}} = \zeta_1^{-1} \frac{1}{n} \sum_{i=1}^n \mathbf{U}_i + \zeta_1^{-1} \boldsymbol{\varrho}$ , where  $\|\boldsymbol{\varrho}\|_2 = O_p(n^{-1})$ . So

$$\begin{aligned} &\frac{2}{n} \sum_{i=1}^n r_i^{-1} [\mathbf{I}_d - \mathbf{U}_i \mathbf{U}_i^T] \hat{\boldsymbol{\theta}} \mathbf{U}_i^T \\ &= \frac{2}{n^2} \sum_{i=1}^n \sum_{j=1}^n \zeta_1^{-1} r_i^{-1} [\mathbf{I}_d - \mathbf{U}_i \mathbf{U}_i^T] \mathbf{U}_j \mathbf{U}_i^T + \frac{2}{n} \sum_{i=1}^n r_i^{-1} \zeta_1^{-1} [\mathbf{I}_d - \mathbf{U}_i \mathbf{U}_i^T] \boldsymbol{\varrho} \mathbf{U}_i^T \\ &= \frac{2}{n^2} \sum_{i=1}^n \sum_{j \neq i}^n \nu_i [\mathbf{I}_d - \mathbf{U}_i \mathbf{U}_i^T] \mathbf{U}_j \mathbf{U}_i^T + \frac{2}{n} \sum_{i=1}^n \nu_i [\mathbf{I}_d - \mathbf{U}_i \mathbf{U}_i^T] \boldsymbol{\varrho} \mathbf{U}_i^T \\ &\doteq B_1 + B_2 \end{aligned}$$

By the Chebyshev inequality, for any  $\mathbf{u} \in \mathbb{S}^{d-1}$ , we have

$$P\left(\frac{2}{n^2} \sum_{i=1}^n \sum_{j \neq i}^n \nu_i \mathbf{u}^T [\mathbf{I}_d - \mathbf{U}_i \mathbf{U}_i^T] \mathbf{U}_j \mathbf{U}_j^T \mathbf{u} \geq \sqrt{18/\alpha} n^{-1} \sigma_v \|\mathbf{S}\|_2\right) \leq \frac{n^{-2} \sigma_v^2 (\mathbf{u}^T \mathbf{S} \mathbf{u})^2}{18 \alpha^{-1} n^{-2} \sigma_v^2 \|\mathbf{S}\|_2^2} \leq \frac{\alpha}{18}.$$

So  $P(\|B_1\| \geq 3\sqrt{2}\alpha^{-1/2} n^{-1} \sigma_v \|\mathbf{S}\|_2) \leq \frac{\alpha}{18}$ . Additionally,

$$\begin{aligned} & \left(\frac{1}{n} \sum_{i=1}^n \mathbf{u}^T \nu_i [\mathbf{I}_d - \mathbf{U}_i \mathbf{U}_i^T] \varrho \mathbf{U}_i^T \mathbf{u}\right)^2 \\ & \leq \left(\frac{1}{n} \sum_{i=1}^n (\mathbf{u}^T [\mathbf{I}_d - \mathbf{U}_i \mathbf{U}_i^T] \varrho)^2\right) \left(\frac{1}{n} \sum_{i=1}^n \nu_i^2 (\mathbf{U}_i^T \mathbf{u})^2\right) \\ & \leq \frac{1}{n} \sum_{i=1}^n \nu_i^2 \|\varrho\|_2^2 = O_p(n^{-2}). \end{aligned}$$

So, for sufficient large  $n$ , there exist a constant  $C_\rho$ , such that  $P(\|B_2\|_2 \geq C_\rho n^{-1}) \leq \frac{\alpha}{18}$ .

Finally, by the triangle inequality, for any  $\alpha > 0$ , there exist a positive constant  $C_S$ , such that, for sufficient large  $n$  and  $\delta \in (0, 1)$ ,

$$\|\hat{\mathbf{S}} - \mathbf{S}\|_2 \leq \|\mathbf{S}\|_2 \sqrt{\frac{4(1+r^*(\mathbf{S}))(\log d + \log(3/\alpha))}{n}} + C_S n^{-\frac{1}{2}(1+\delta)}$$

with probability larger than  $1 - \alpha$ . □

### 7.2.3 Proof of Corollary 2.1

The Davis-Kahan inequality states that the approximation error of  $\mathbf{u}_1(\hat{\mathbf{S}})$  to  $\mathbf{u}_1(\mathbf{S})$  is controlled by  $\|\hat{\mathbf{S}} - \mathbf{S}\|_2$  divided by the eigengap between  $\lambda_1(\mathbf{S})$  and  $\lambda_2(\mathbf{S})$ :

$$\left|\sin \angle \left(\mathbf{u}_1(\hat{\mathbf{S}}), \mathbf{u}_1(\mathbf{S})\right)\right| \leq \frac{2}{\lambda_1(\mathbf{S}) - \lambda_2(\mathbf{S})} \|\hat{\mathbf{S}} - \mathbf{S}\|_2.$$

Thus, by Theorem 2.1, we can directly obtain the result. □

### 7.2.4 Proof of Theorem 3.1

**LEMMA 7.5** *Suppose that  $\mathbf{X} \sim EC_d(\boldsymbol{\mu}, \boldsymbol{\Sigma}, \xi)$  is elliptically distributed. For any  $\mathbf{v} \in \mathbb{S}^{d-1}$ , suppose that*

$$E \exp\left(t \left[ (\mathbf{v}^T U(\mathbf{X}))^2 - \mathbf{v}^T \mathbf{S} \mathbf{v} \right]\right) \leq \exp(\eta t^2), \quad \text{for } t \leq c_0/\sqrt{\eta} \quad (10)$$

where  $\eta > 0$  only depends on the eigenvalues of  $\Sigma$  and  $c_0$  is an absolute constant. We then have, with probability no smaller than  $1 - 2\alpha$ , for large enough  $n$ ,

$$\sup_{\mathbf{v} \in \mathbb{S}^{d-1} \cap \mathbb{B}_0(s)} \left| \mathbf{v}^T (\tilde{\mathbf{S}} - \mathbf{S}) \mathbf{v} \right| \leq 4\eta^{1/2} \sqrt{\frac{s(3 + \log(d/s)) + \log(1/\alpha)}{n}}$$

**Proof:** Let  $a \in \mathbb{Z}^+$  be an integer no smaller than 1 and  $J_a$  be any subset of  $\{1, \dots, d\}$  with cardinality  $a$ . For any  $s$ -dimensional sphere  $\mathbb{S}^{s-1}$  equipped with Euclidean distance, we let  $\mathcal{N}_\epsilon$  be a subset of  $\mathbb{S}^{s-1}$  such that for any  $\mathbf{v} \in \mathbb{S}^{s-1}$ , there exists  $\mathbf{u} \in \mathcal{N}_\epsilon$  subject to  $\|\mathbf{u} - \mathbf{v}\|_2 \leq \epsilon$ . It is known that the cardinal number of  $\mathcal{N}_\epsilon$  has an upper bound:  $\text{card}(\mathcal{N}_\epsilon) < (1 + \frac{2}{\epsilon})^s$ . Let  $\mathcal{N}_{1/4}$  be a  $(1/4)$ -net of  $\mathbb{S}^{s-1}$ . We then have  $\text{card}(\mathcal{N}_{1/4})$  is upper bounded by  $9^s$ . Moreover, for any symmetric matrix  $\mathbf{M} \in \mathbb{R}^{s \times s}$ , we have

$$\sup_{\mathbf{v} \in \mathbb{S}^{s-1}} |\mathbf{v}^T \mathbf{M} \mathbf{v}| \leq \frac{1}{1 - 2\epsilon} \sup_{\mathbf{v} \in \mathcal{N}_\epsilon} |\mathbf{v}^T \mathbf{M} \mathbf{v}|, \text{ implying } \sup_{\mathbf{v} \in \mathbb{S}^{s-1}} |\mathbf{v}^T \mathbf{M} \mathbf{v}| \leq 2 \sup_{\mathbf{v} \in \mathcal{N}_{1/4}} |\mathbf{v}^T \mathbf{M} \mathbf{v}|$$

Let  $\beta > 0$  be a quantity defined as  $\beta := (8\eta)^{1/2} \sqrt{\frac{s(3 + \log(d/s)) + \log(1/\alpha)}{n}}$ . By the union bound, we have

$$\begin{aligned} & P \left( \sup_{\mathbf{b} \in \mathbb{S}^{s-1}} \sup_{J_s \subset \{1, \dots, d\}} \left| \mathbf{b}^T [\tilde{\mathbf{S}} - \mathbf{S}]_{J_s, J_s} \mathbf{b} \right| > 2\beta \right) \leq P \left( \sup_{\mathbf{b} \in \mathcal{N}_{1/4}} \sup_{J_s \subset \{1, \dots, d\}} \left| \mathbf{b}^T [\tilde{\mathbf{S}} - \mathbf{S}]_{J_s, J_s} \mathbf{b} \right| > \beta \right) \\ & \leq 9^s \binom{d}{s} P \left( \left| \mathbf{b}^T [\tilde{\mathbf{S}} - \mathbf{S}]_{J_s, J_s} \mathbf{b} \right| > (8\eta)^{1/2} \sqrt{\frac{s(3 + \log(d/s)) + \log(1/\alpha)}{n}}, \text{ for any } \mathbf{b} \text{ and } J_s \right) \end{aligned}$$

Thus, if we can show that for any  $\mathbf{b} \in \mathbb{S}^{s-1}$  and  $J_s$ , we have

$$P \left( \left| \mathbf{b}^T [\tilde{\mathbf{S}} - \mathbf{S}]_{J_s, J_s} \mathbf{b} \right| > t \right) \leq 2e^{-nt^2/(4\eta)} \quad (11)$$

for  $\eta$  defined in Equation (10). Then, using the bound  $\binom{d}{s} < (ed/s)^s$ , we have

$$9^s \binom{d}{s} P \left( \left| \mathbf{b}^T [\tilde{\mathbf{S}} - \mathbf{S}]_{J_s, J_s} \mathbf{b} \right| > (4\eta)^{1/2} \sqrt{\frac{s(3 + \log(d/s)) + \log(1/\alpha)}{n}}, \text{ for any } \mathbf{b} \text{ and } J \right) \leq 2\alpha.$$

In fact, by the assumption (10) and Markov inequality, we have

$$\begin{aligned}
& P\left(\mathbf{b}^T[\tilde{\mathbf{S}} - \mathbf{S}]_{J_s, J_s} \mathbf{b} > t\right) \leq E\left(e^{-nt^2/(2\eta)} \exp\left[tn/(2\eta)\mathbf{b}^T[\tilde{\mathbf{S}} - \mathbf{S}]_{J_s, J_s} \mathbf{b}\right]\right) \\
& = e^{-nt^2/(2\eta)} E\left(\exp\left[tn/(2\eta)\mathbf{b}^T\left[\frac{1}{n}\sum_{i=1}^T \mathbf{U}_i \mathbf{U}_i^T - \mathbf{S}\right]_{J_s, J_s} \mathbf{b}\right]\right) \\
& = e^{-nt^2/(2\eta)} \left\{E(\exp((2\eta)^{-1}t\mathbf{b}^T[\mathbf{U}_i \mathbf{U}_i^T - \mathbf{S}]_{J_s, J_s} \mathbf{b}))\right\}^n \\
& \leq e^{-nt^2/(2\eta)} \left\{E(\exp((2\eta)^{-1}t\mathbf{u}^T[\mathbf{U}_i \mathbf{U}_i^T - \mathbf{S}]\mathbf{u}))\right\}^n \\
& \leq e^{-nt^2/(2\eta)} e^{(4\eta)^{-1}nt^2} \leq e^{-nt^2/(4\eta)}
\end{aligned}$$

for  $t \leq c_0\eta^{1/2}$ . By symmetry, we can easily obtain the result (11).

**Proof of Theorem 3.1:** Note that  $U(\mathbf{X})$  has the same distribution as  $S(X) = \frac{\mathbf{x} - \tilde{\mathbf{X}}}{\|\mathbf{x} - \tilde{\mathbf{X}}\|}$  where  $\mathbf{X}, \tilde{\mathbf{X}} \sim EC_d(\boldsymbol{\mu}, \boldsymbol{\Sigma}, \xi)$  and are independent. By Lemma B.4 in Han and Liu (2018), for any  $\mathbf{v} = (v_1, \dots, v_d)^T \in \mathbb{S}^{d-1}$ , Equation (10) holds with

$$\eta = \sup_{\mathbf{v} \in \mathbb{S}^{d-1}} 2 \|\mathbf{v}^T U(\mathbf{X})\|_{\psi_2}^2 + \|\mathbf{K}\|_2$$

and

$$\sup_{\mathbf{v} \in \mathbb{S}^{d-1}} \|\mathbf{v}^T U(\mathbf{X})\|_{\psi_2} = \sup_{\mathbf{v} \in \mathbb{S}^{d-1}} \left\| \frac{\sum_{i=1}^d v_i \lambda_i^{1/2}(\boldsymbol{\Sigma}) Y_i}{\sqrt{\sum_{i=1}^d \lambda_i(\boldsymbol{\Sigma}) Y_i^2}} \right\|_{\psi_2}$$

where  $(Y_1, \dots, Y_d)^T \sim N_d(\mathbf{0}, \mathbf{I}_d)$  is standard Gaussian. Thus, by Lemma 7.5, when  $(s \log(ed/s) + \log(1/\alpha))/n \rightarrow 0$ , with probability at least  $1 - 2\alpha$ , we have

$$\|\tilde{\mathbf{S}} - \mathbf{S}\|_{2,s} \leq C_0 \left( \sup_{\mathbf{v} \in \mathbb{S}^{d-1}} 2 \|\mathbf{v}^T U(\mathbf{X})\|_{\psi_2}^2 + \|\mathbf{S}\|_2 \right) \sqrt{\frac{s(3 + \log(d/s)) + \log(1/\alpha)}{n}}.$$

Taking the same procedure as Lemma 7.4, we can have  $\|\hat{\boldsymbol{\theta}}\|_{2,s} = O_p(\sqrt{\frac{s}{d}} \zeta_1^{-1} n^{-1/2})$ . So taking the same procedure as the proof of Theorem 2.1, we have, there exist some positive constant  $C_1 > 0$ ,

$$\|\hat{\mathbf{S}} - \tilde{\mathbf{S}}\|_{2,s} \leq C_1 \left(\frac{nd}{s}\right)^{-\frac{1}{2}(1+\delta)}$$

for sufficient large  $n$  and with probability larger than  $1 - \alpha$ . Then, by the triangle inequality, we obtain the first result. Specially, if  $\text{rank}(\boldsymbol{\Sigma}) = q$  and  $\|\mathbf{u}_1(\boldsymbol{\Sigma})\|_0 \leq s$ , by Theorem 4.2 in

citehan2018eca, we have

$$\sup_{\mathbf{v} \in \mathbb{S}^{d-1}} \|\mathbf{v}^T U(\mathbf{X})\|_{\psi_2} \leq \sqrt{\frac{\lambda_1(\boldsymbol{\Sigma})}{\lambda_q(\boldsymbol{\Sigma})} \cdot \frac{2}{q}} \wedge 1.$$

So we can easily obtain the second result.  $\square$

### 7.2.5 Proof of Corollary 3.1

The Davis-Kahan inequality and Theorem 3.1, we can directly obtain the result.  $\square$

### 7.2.6 Proof of Theorem 7.1

Using the result in Theorem 3.1, we have for any  $\mathbf{v} \in \mathbb{S}^{d-1}$ ,

$$\|\mathbf{v}^T U(\mathbf{X})\|_{\psi_2} \leq \sqrt{\frac{\lambda_1(\boldsymbol{\Sigma})}{\lambda_q(\boldsymbol{\Sigma})} \cdot \frac{2}{q}}. \quad (12)$$

So, for any  $j, k \in \{1, \dots, d\}$ , we have

$$\|\mathbf{e}_j^T U(\mathbf{X}_i) U(\mathbf{X}_i)^T \mathbf{e}_k\|_{\psi_1} \leq \frac{\lambda_1(\boldsymbol{\Sigma})}{\lambda_q(\boldsymbol{\Sigma})} \cdot \frac{8}{q}$$

where  $\mathbf{e}_j = (0, \dots, 0, 1, 0, \dots, 0)$  with the  $j$ -th element being one and the others are zeros.

So by the Bernstein inequality, we have

$$P(|\mathbf{e}_j^T U(\mathbf{X}_i) U(\mathbf{X}_i)^T \mathbf{e}_k - \mathbf{S}_{jk}| \geq t) \leq \exp\left(-\frac{nt^2}{8C(8(\lambda_1(\boldsymbol{\Sigma})/q\lambda_q(\boldsymbol{\Sigma})) + \mathbf{S}_{jk})^2}\right)$$

for  $t < 2Cc(8\lambda_1(\boldsymbol{\Sigma})/q\lambda_q(\boldsymbol{\Sigma}) + \mathbf{K}_{jk})$ . So,

$$P(\|\tilde{\mathbf{S}} - \mathbf{S}\|_{\max} \geq t) \leq d^2 \exp\left(-\frac{nt^2}{8C(8\lambda_1(\boldsymbol{\Sigma})/q\lambda_q(\boldsymbol{\Sigma}) + \|\mathbf{S}\|_{\max})^2}\right).$$

Then, with probability larger than  $1 - \alpha^2$ , for sufficient large  $n$ , we have

$$\|\tilde{\mathbf{S}} - \mathbf{S}\|_{\max} \leq 4\sqrt{C} \left( \frac{8\lambda_1(\boldsymbol{\Sigma})}{q\lambda_q(\boldsymbol{\Sigma})} + \|\mathbf{S}\|_{\max} \right) \sqrt{\frac{\log d + \log(1/\alpha)}{n}}.$$



Next, we will show the bound of  $\|\hat{\mathbf{S}} - \tilde{\mathbf{S}}\|_{max}$ . Because

$$\begin{aligned}\hat{\mathbf{S}} - \tilde{\mathbf{S}} &= \frac{1}{n} \sum_{i=1}^n [\hat{\mathbf{U}}_i \hat{\mathbf{U}}_i^T - \mathbf{U}_i \mathbf{U}_i^T] \\ &= \frac{2}{n} \sum_{i=1}^n [\hat{\mathbf{U}}_i - \mathbf{U}_i] \mathbf{U}_i^T + \frac{1}{n} \sum_{i=1}^n [\hat{\mathbf{U}}_i - \mathbf{U}_i] [\hat{\mathbf{U}}_i - \mathbf{U}_i]^T \doteq J_1 + J_2\end{aligned}$$

Because

$$\begin{aligned}\hat{\mathbf{U}}_i - \mathbf{U}_i &= \frac{\mathbf{X}_i - \hat{\boldsymbol{\mu}}}{\|\mathbf{X}_i - \hat{\boldsymbol{\mu}}\|} - \frac{\mathbf{X}_i - \boldsymbol{\mu}}{\|\mathbf{X}_i - \boldsymbol{\mu}\|} \\ &= \frac{\mathbf{X}_i - \hat{\boldsymbol{\mu}}}{\|\mathbf{X}_i - \hat{\boldsymbol{\mu}}\|} - \frac{\mathbf{X}_i - \hat{\boldsymbol{\mu}}}{\|\mathbf{X}_i - \boldsymbol{\mu}\|} + \frac{\mathbf{X}_i - \hat{\boldsymbol{\mu}}}{\|\mathbf{X}_i - \boldsymbol{\mu}\|} - \frac{\mathbf{X}_i - \boldsymbol{\mu}}{\|\mathbf{X}_i - \boldsymbol{\mu}\|} \\ &= (\mathbf{X}_i - \hat{\boldsymbol{\mu}})(\hat{r}_i^{-1} - r_i^{-1}) + (\hat{\boldsymbol{\mu}} - \boldsymbol{\mu})r_i^{-1} \\ &= \mathbf{U}_i(r_i \hat{r}_i^{-1} - 1) + (\hat{\boldsymbol{\mu}} - \boldsymbol{\mu})(\hat{r}_i^{-1} - r_i^{-1}) + (\hat{\boldsymbol{\mu}} - \boldsymbol{\mu})r_i^{-1}.\end{aligned}$$

So

$$\begin{aligned}\left\| \frac{J_1}{2} \right\|_{max} &\leq \left\| \frac{1}{n} \sum_{i=1}^n (r_i \hat{r}_i^{-1} - 1) \mathbf{U}_i \mathbf{U}_i^T \right\|_{max} + \left\| \frac{1}{n} \sum_{i=1}^n (\hat{r}_i^{-1} - r_i^{-1}) (\hat{\boldsymbol{\mu}} - \boldsymbol{\mu}) \mathbf{U}_i^T \right\|_{max} \\ &\quad + \left\| \frac{1}{n} \sum_{i=1}^n (\hat{\boldsymbol{\mu}} - \boldsymbol{\mu}) r_i^{-1} \mathbf{U}_i^T \right\|_{max} \\ &\doteq J_{11} + J_{12} + J_{13}.\end{aligned}$$

First,

$$J_{11} \leq \max_{1 \leq i \leq T} |r_i \hat{r}_i^{-1} - 1| \|\tilde{\mathbf{S}}\|_{max}.$$

Because  $|\hat{r}_i - r_i| \leq \|\hat{\boldsymbol{\mu}} - \boldsymbol{\mu}\|$ , so  $|r_i \hat{r}_i^{-1} - 1| \leq \frac{\|\hat{\boldsymbol{\mu}} - \boldsymbol{\mu}\|}{r_i - \|\hat{\boldsymbol{\mu}} - \boldsymbol{\mu}\|}$ . Then,

$$\max_{1 \leq i \leq T} |r_i \hat{r}_i^{-1} - 1| \leq \zeta_1 \|\hat{\boldsymbol{\mu}} - \boldsymbol{\mu}\| \max_{1 \leq i \leq T} (\zeta_1 r_i - \zeta_1 \|\hat{\boldsymbol{\mu}} - \boldsymbol{\mu}\|)^{-1}.$$

By Lemma 7.4, we have  $\zeta_1 \|\hat{\boldsymbol{\mu}} - \boldsymbol{\mu}\| = O_p(n^{-1/2})$ . And by the sub-gaussian assumption of  $\nu_i$ , we have  $\max_{1 \leq i \leq n} \nu_i = O_p(\log^{1/2} n)$ . So  $\max_{1 \leq i \leq T} |r_i \hat{r}_i^{-1} - 1| = O_p(\sqrt{\frac{\log n}{n}})$ . In addition  $\|\tilde{\mathbf{S}}\|_{max} \leq \|\tilde{\mathbf{S}} - \mathbf{S}\|_{max} + \|\mathbf{S}\|_{max}$ . So, with probability larger than  $1 - \alpha$ ,

$$J_{11} \leq C \sqrt{\frac{\log n}{n}} \left( \|\mathbf{S}\|_{max} + 4\sqrt{C} \left( \frac{8\lambda_1(\boldsymbol{\Sigma})}{q\lambda_q(\boldsymbol{\Sigma})} + \|\mathbf{S}\|_{max} \right) \sqrt{\frac{\log d + \log(1/\alpha)}{n}} \right)$$

for sufficient large  $C$  and  $n$ .

Obviously,

$$J_{13} \leq \zeta_1 \|\hat{\boldsymbol{\mu}} - \boldsymbol{\mu}\|_\infty \left\| \frac{1}{n} \sum_{i=1}^T \nu_i \mathbf{U}_i \right\|_\infty.$$

By (12) and  $\nu_i$  is also sub-gaussian variable with parameter  $K_\nu$ , we have

$$\|\nu_i \mathbf{U}_i^T \mathbf{v}\|_{\psi_1} \leq \|\nu_i\|_{\psi_2} \|\mathbf{U}_i^T \mathbf{v}\|_{\psi_2} \leq K_\nu \sqrt{\frac{\lambda_1(\boldsymbol{\Sigma})}{\lambda_q(\boldsymbol{\Sigma})}} \cdot \frac{2}{q}.$$

So, by the Bernstein inequality, we have

$$P\left(\frac{1}{n} \sum_{i=1}^T \nu_i \mathbf{U}_i^T e_k \geq t\right) \leq \exp\left(-\frac{nt^2}{8CK_\nu^2 \lambda_1(\boldsymbol{\Sigma})/q\lambda_q(\boldsymbol{\Sigma})}\right)$$

for  $t \leq cK_\nu \sqrt{\lambda_1(\boldsymbol{\Sigma})/q\lambda_q(\boldsymbol{\Sigma})}$  for some positive constant  $c, C$ . Then,

$$P\left(\left\|\frac{1}{n} \sum_{i=1}^T \nu_i \mathbf{U}_i\right\|_\infty \geq t\right) \leq d \exp\left(-\frac{nt^2}{8CK_\nu^2 \lambda_1(\boldsymbol{\Sigma})/q\lambda_q(\boldsymbol{\Sigma})}\right) \leq \alpha$$

by setting  $t = \sqrt{\frac{8CK_\nu^2 \lambda_1(\boldsymbol{\Sigma})}{q\lambda_q(\boldsymbol{\Sigma})}} \sqrt{\frac{\log d + \log(1/\alpha)}{n}}$ . Similar to the above arguments, we have

$$P\left(\left\|\frac{1}{n} \sum_{i=1}^T \mathbf{U}_i\right\|_\infty \geq \sqrt{\frac{8C\lambda_1(\boldsymbol{\Sigma})}{q\lambda_q(\boldsymbol{\Sigma})}} \sqrt{\frac{\log d + \log(1/\alpha)}{n}}\right) \leq \alpha.$$

By the equation  $\sum_{i=1}^n \hat{\mathbf{U}}_i = 0$ , we have

$$\begin{aligned} \zeta_1(\hat{\boldsymbol{\mu}} - \boldsymbol{\mu}) &= \frac{1}{n} \sum_{i=1}^n \mathbf{U}_i + \frac{1}{n} \sum_{i=1}^n (r_i \hat{r}_i^{-1} - 1) \mathbf{U}_i + \left(\frac{\zeta_1}{\frac{1}{n} \sum_{i=1}^n \hat{r}_i^{-1}} - 1\right) \frac{1}{n} \sum_{i=1}^n \mathbf{U}_i \\ &\quad + \left(\frac{\zeta_1}{\frac{1}{n} \sum_{i=1}^n \hat{r}_i^{-1}} - 1\right) \frac{1}{n} \sum_{i=1}^n \mathbf{U}_i (r_i \hat{r}_i^{-1} - 1) \\ &\doteq B_1 + B_2 + B_3 + B_4. \end{aligned}$$

By the sub-gaussian assumption of  $\nu_i$ , we have  $\|B_i\|_\infty = O_p\left(\sqrt{\frac{\log n}{n}}\right) \|B_1\|_\infty$ ,  $i = 2, 3, 4$ . So

$$\zeta_1 \|\hat{\boldsymbol{\mu}} - \boldsymbol{\mu}\|_\infty \leq \sqrt{\frac{9C\lambda_1(\boldsymbol{\Sigma})}{q\lambda_q(\boldsymbol{\Sigma})}} \sqrt{\frac{\log d + \log(1/\alpha)}{n}}$$

with probability larger than  $1 - \alpha$  for sufficient large  $n$  and  $C$ . Then,

$$J_{13} \leq \frac{C\lambda_1(\boldsymbol{\Sigma}) \log d + \log(1/\alpha)}{q\lambda_q(\boldsymbol{\Sigma}) n}$$

with probability larger than  $1 - 2\alpha$  for sufficient large  $n$  and  $C$ . Finally,

$$J_{12} \leq \max_{1 \leq i \leq T} |r_i \hat{r}_i^{-1} - 1| J_{13}$$

which implies  $J_{12}$  is a smaller order than  $J_{13}$ . So, by the triangle inequality, we obtain that  $\|J_1\|_{max} = o_p(\|\tilde{\mathbf{S}} - \mathbf{S}\|_{max})$ . Similarly, we also can prove that  $\|J_2\|_{max} = o_p(\|\tilde{\mathbf{S}} - \mathbf{S}\|_{max})$ . So, we have

$$\|\hat{\mathbf{S}} - \mathbf{S}\|_{max} \leq C \left( \frac{8\lambda_1(\boldsymbol{\Sigma})}{q\lambda_q(\boldsymbol{\Sigma})} + \|\mathbf{S}\|_{max} \right) \sqrt{\frac{\log d + \log(1/\alpha)}{n}}.$$

with probability larger than  $1 - \alpha^2$ . The rest proves are all similar to the proof of Theorem 5.3, Corollary 5.3 and Theorem 5.4 in Han and Liu (2018). So we omit the details here.  $\square$

## References

- Arcones, M. (1998). Asymptotic theory for m-estimators over a convex kernel. *Econometric Theory*, 14:387–422.
- Bai, Z., Chen, R., Miao, B., and Rao, C. (1990). Asymptotic theory of least distances estimate in multivariate linear models. *Statistics*, 4:503–519.
- Baik, J. and Silverstein, J. W. (2006). Eigenvalues of large sample covariance matrices of spiked population models. *Journal of Multivariate Analysis*, 97:1382–1408.
- Bickel, P. and Levina, E. (2008). Regularized estimation of large covariance matrices. *The Annals of Statistics*, 36:199–227.
- Birnbaum, A., Johnstone, I. M., Nadler, B., and Paul, D. (2013). Minimax bounds for sparse pca with noisy high-dimensional data. *The Annals of statistics*, 41:1055–1084.

- Cai, T. T., Ma, Z., and Wu, Y. (2013). Sparse pca: Optimal rates and adaptive estimation. *The Annals of Statistics*, 41:3074–3110.
- Chen, X., Zhang, J., and Zhou, W. (2022). High-dimensional elliptical sliced inverse regression in non-gaussian distributions. *Journal of Business & Economic Statistics*, 40(3):1204–1215.
- Cheng, G., Liu, B., Peng, L., Zhang, B., and Zheng, S. (2019). Testing the equality of two high-dimensional spatial sign covariance matrices. *Scandinavian Journal of Statistics*, 46(1):257–271.
- Croux, C., Filzmoser, P., and Fritz, H. (2013). Robust sparse principal component analysis. *Technometrics*, 55:202–214.
- Croux, C., Ollila, E., and Oja, H. (2002). Sign and rank covariance matrices: Statistical properties and application to principal components analysis. *Statistics for Industry and Technology*, pages 257–269.
- Davis, C. and Kahan, W. M. (1970). The rotation of eigenvectors by a perturbation. iii. *SIAM Journal on Numerical Analysis*, 7:1–46.
- Fan, J., Fan, Y., and Lv, J. (2008). High dimensional covariance matrix estimation using a factor model. *Journal of Econometrics*, 147:186–197.
- Feng, L. (2018). Power comparison between high dimensional t-test, sign, and signed rank tests. *arXiv preprint arXiv:1812.10625*.
- Feng, L. and Liu, B. (2017). High-dimensional rank tests for sphericity. *Journal of Multivariate Analysis*, 155:217–233.
- Feng, L., Liu, B., and Ma, Y. (2021). An inverse norm sign test of location parameter for high-dimensional data. *Journal of Business & Economic Statistics*, 39(3):807–815.
- Feng, L. and Sun, F. (2016). Spatial-sign based high-dimensional location test. *Electronic Journal of Statistics*, 10:2420–2434.

- Feng, L., Zou, C., and Wang, Z. (2016). Multivariate-sign-based high-dimensional tests for the two-sample location problem. *Journal of the American Statistical Association*, 111(514):721–735.
- Han, F. and Liu, H. (2014). Scale-invariant sparse pca on high-dimensional meta-elliptical data. *Journal of the American Statistical Association*, 109:275–287.
- Han, F. and Liu, H. (2018). Eca: High-dimensional elliptical component analysis in non-gaussian distributions. *Journal of the American Statistical Association*, 113(521):252–268.
- He, Y., Kong, X., Yu, L., and Zhang, X. (2022). Large-dimensional factor analysis without moment constraints. *Journal of Business & Economic Statistics*, 40(1):302–312.
- Huang, X., Liu, B., Zhou, Q., and Feng, L. (2023). A high-dimensional inverse norm sign test for two-sample location problems. *Canadian Journal of Statistics*, 51(4):1004–1033.
- Hubert, M., Reynkens, T., Schmitt, E., and Verdonck, T. (2016). Sparse pca for high-dimensional data with outliers. *Technometrics*, 58(4):424–434.
- Hubert, M., Rousseeuw, P. J., and Vanden Branden, K. (2005). Robpca: a new approach to robust principal component analysis. *Technometrics*, 47(1):64–79.
- Johnstone, I. M. and Lu, A. Y. (2009). On consistency and sparsity for principal components analysis in high dimensions. *Journal of the American Statistical Association*, 104:682–693.
- Jolliffe, I., Trendafilov, N., and Uddin, M. (2003). A modified principal component technique based on the lasso. *Journal of Computational and Graphical Statistics*, 12:531–547.
- Journee, M., Nesterov, Y., Richtarik, P., and Sepulchre, R. (2010). Generalized power method for sparse principal component analysis. *Journal of Machine Learning Research*, 11:517–553.
- Li, W. and Xu, Y. (2022). Asymptotic properties of high-dimensional spatial median in elliptical distributions with application. *Journal of Multivariate Analysis*, 190:104975.

- Liu, B., Feng, L., and Ma, Y. (2023). High-dimensional alpha test of linear factor pricing models with heavy-tailed distributions. *Statistica Sinica*, 33:1389–1410.
- Locantore, N., Marron, J., Simpson, D., Tripoli, N., Zhang, J., Cohen, K., Boente, G., Fraiman, R., Brumback, B., Croux, C., et al. (1999). Robust principal component analysis for functional data. *Test*, 8:1–73.
- Lounici, K. (2014). High-dimensional covariance matrix estimation with missing observations. *Bernoulli*, 20:1029–1058.
- Ma, Z. (2013). Sparse principal component analysis and iterative thresholding. *The Annals of Statistics*, 41:772–801.
- Mackey, L. (2008). Deflation methods for sparse pca. In *Advances in Neural Information Processing Systems*, volume 21, pages 1017–1024.
- Marden, J. (1999). Some robust estimates of principal components. *Statistics and Probability Letters*, 43:349–359.
- Nadler, B. (2008). Finite sample approximation results for principal component analysis: A matrix perturbation approach. *The Annals of Statistics*, 36:2791–2817.
- Neter, J., Kutner, M., Wasserman, W., and Nachtsheim, C. (1996). *Applied Linear Statistical Models*, volume 4. Irwin, Chicago, IL.
- Oja, H. (2010). *Multivariate Nonparametric Methods with R: An Approach based on Spatial Signs and Ranks*, volume 199. Springer, New York.
- Paindaveine, D. and Verdebout, T. (2016). On high-dimensional sign tests. *Bernoulli*, 22(3):1745–1769.
- Paul, D. (2007). Asymptotics of sample eigenstructure for a large dimensional spiked covariance model. *Statistica Sinica*, pages 1617–1642.

- Shen, H. and Huang, J. Z. (2008). Sparse principal component analysis via regularized low rank matrix approximation. *Journal of multivariate analysis*, 99:1015–1034.
- Taskinen, S., Koch, I., and Oja, H. (2012). Robustifying principal component analysis with spatial sign vectors. *Statistics and Probability Letters*, 82:765–774.
- Tropp, J. A. (2012). User-friendly tail bounds for sums of random matrices. *Foundations of Computational Mathematics*, 12:389–434.
- Vershynin, R. (2010). *Introduction to the Non-Asymptotic Analysis of Random Matrices*, pages 210–268. Cambridge University Press.
- Visuri, S., Koivunen, V., and Oja, H. (2000). Sign and rank covariance matrices. *Journal of Statistical Planning and Inference*, 91(2):557–575.
- Vu, V. and Lei, J. (2012). Minimax rates of estimation for sparse pca in high dimensions. In *Proceedings of the 15th International Conference on Artificial Intelligence and Statistics (AISTATS)*, volume 22, pages 1278–1286.
- Vu, V. Q., Cho, J., Lei, J., and Rohe, K. (2013). Fantope projection and selection: A near-optimal convex relaxation of sparse pca. In *Advances in Neural Information Processing Systems*, volume 26, pages 2670–2678.
- Vu, V. Q. and Lei, J. (2013). Minimax sparse principal subspace estimation in high dimensions. *The Annals of Statistics*, 41:2905–2947.
- Wang, L., Peng, B., and Li, R. (2015). A high-dimensional nonparametric multivariate test for mean vector. *Journal of the American Statistical Association*, 110(512):1658–1669.
- Wang, Z., Han, F., and Liu, H. (2013). Sparse principal component analysis for high dimensional vector autoregressive models. *arXiv:1307.0164*.
- Wedin, P.-A. (1972). Perturbation bounds in connection with singular value decomposition. *BIT Numerical Mathematics*, 12:99–111.

- Witten, D. M., Tibshirani, R., and Hastie, T. (2009). A penalized matrix decomposition, with applications to sparse principal components and canonical correlation analysis. *Biostatistics*, 10:515–534.
- Yuan, X. and Zhang, T. (2013). Truncated power method for sparse eigenvalue problems. *Journal of Machine Learning Research*, 14:899–925.
- Zhang, X., Zhao, P., and Feng, L. (2022). Robust sphericity test in the panel data model. *Statistics & Probability Letters*, 182:109304.
- Zhang, Y. and El Ghaoui, L. (2011). Large-scale sparse principal component analysis with application to text data. In *Advances in Neural Information Processing Systems*, volume 24, pages 532–539.
- Zhao, P., Chen, D., and Wang, Z. (2023). Spatial-sign based high dimensional white noises test. *arXiv preprint arXiv:2303.10641*.
- Zou, C., Peng, L., Feng, L., and Wang, Z. (2014). Multivariate sign-based high-dimensional tests for sphericity. *Biometrika*, 101(1):229–236.
- Zou, H., Hastie, T., and Tibshirani, R. (2006). Sparse principal component analysis. *Journal of computational and graphical statistics*, 15:265–286.
- Zou, H. and Xue, L. (2018). A selective overview of sparse principal component analysis. *Proceedings of the IEEE*, 106:1311–1320.